NASA Technical Paper 1890

Effect of Simulated In-Flight Thrust Reversing on Vertical-Tail Loads of F-18 and F-15 Airplane Models

E. Ann Bare, Bobby L. Berrier,
and Francis J. Capone

AUGUST 1981

NASA

NASA Technical Paper 1890

Effect of Simulated In-Flight Thrust Reversing on Vertical-Tail Loads of F-18 and F-15 Airplane Models

E. Ann Bare, Bobby L. Berrier,
and Francis J. Capone
Langley Research Center
Hampton, Virginia

National Aeronautics
and Space Administration

**Scientific and Technical
Information Branch**

1981

SUMMARY

Investigations were conducted in the Langley 16-Foot Transonic Tunnel to provide data on the effect of simulated in-flight thrust reversing on vertical-tail loads of a 0.10-scale model of the prototype F-18 airplane and a 0.047-scale model of the F-15 three-surface configuration (canard, wing, and horizontal tails). Test data were obtained at static conditions and at Mach numbers from 0.6 to 1.2 over an angle-of-attack range from -2° to 15°. Nozzle pressure ratio was varied from jet off to about 8.0.

The use of an in-flight thrust reverser with twin-vertical-tail configurations at subsonic Mach numbers increases the pressure on the inboard side of the vertical tail and thus tends to produce an outward side force on the vertical tails. The estimated vertical-tail side-force loads on the F-15 are greater in magnitude than the side-force loads measured on the F-18 vertical tails. Operation of the thrust reverser at Mach 1.2 had no effect on the F-18 vertical-tail side-force coefficients.

INTRODUCTION

Recent studies on twin-engine fighter aircraft (refs. 1 to 5) have identified potential benefits for nonaxisymmetric nozzles in place of conventional axisymmetric or round nozzles. One primary benefit of the nonaxisymmetric nozzle is its versatility which allows inclusion of thrust vectoring and reversing capabilities with less weight penalty than on a conventional axisymmetric nozzle (refs. 5 and 6). Since field length of current high thrust-to-weight fighter airplanes is fixed by landing distance as opposed to take-off distance, addition of thrust reversing capability would greatly enhance short-field landing performance of most current and future fighter aircraft. In addition, use of in-flight thrust reversing during air-to-air combat has the potential to improve airplane agility (prevent or cause over-shoot) and to cause break lock of aggressor missiles (refs. 7 and 8).

Several recent wind-tunnel investigations (refs. 9 to 13) to determine the performance of nonaxisymmetric nozzle thrust reversers at static and subsonic flight conditions indicate that highly efficient thrust reversers can be designed. However, use of an in-flight thrust reverser could cause additional loads on airplane tail surfaces, particularly on twin-vertical-tail configurations which will probably experience differential pressures on the inboard and outboard panels of each vertical tail. For twin-vertical-tail configurations, the reverse exhaust flow is generally directed between the vertical tails, and substantial interaction with the free-stream flow is expected in this region at forward flight conditions. Since the tail load on each vertical tail is expected to be nearly equal but opposite in direction, little information can be obtained concerning tail loads from conventional force and moment wind-tunnel tests; tail static-pressure measurements or special test techniques are required to obtain tail load information.

This paper presents the effect of simulated in-flight thrust reversing on the vertical-tail loads of scale models of the F-15 and F-18 airplanes. Both configurations had twin vertical tails and installed nonaxisymmetric nozzles. The investigation was conducted in the Langley 16-Foot Transonic Tunnel at Mach numbers from 0.6 to 1.2 and nozzle pressure ratios from 1.0 (jet off) to about 8.0. Tests were conducted at conditions of normal cruise flight and full reverse thrust (reverser fully deployed). The effects of installing nonaxisymmetric nozzles with thrust reversers on the aerodynamic characteristics of the F-15 airplane and the F-18 airplane are presented in references 12 and 13, respectively.

SYMBOLS

A_e nozzle exit area, cm^2

A_t nozzle throat area, cm^2

C_p pressure coefficient, $\dfrac{p_l - p_\infty}{q_\infty}$

ΔC_p incremental pressure coefficient, $(C_p)_{outboard} - (C_p)_{inboard}$

C_Y total side-force coefficient, $\dfrac{\text{Total side force}}{q_\infty S}$

ΔC_Y incremental side-force coefficient, $(C_Y)_{R/H\ vertical\ tail\ only} - (C_Y)_{vertical\ tails\ off}$

$C_{Y,tail}$ vertical-tail side-force coefficient (one tail), $\dfrac{\text{Vertical-tail side force}}{q_\infty S}$

$C_{Y,v}$ vertical-tail side-force coefficient from yawing moment, $\dfrac{\text{Yawing moment}}{\text{Vertical-tail moment arm}}$

c local vertical-tail chord, cm

$\bar{c}$ wing mean geometric chord, cm

M free-stream Mach number

p_l local static pressure, Pa

$p_{t,j}$ average jet total pressure, Pa

p_∞ free-stream static pressure, Pa

q_∞ free-stream dynamic pressure, Pa

S wing reference area, 3716.2 cm^2 for F-18 and 1244.9 cm^2 for F-15

x axial distance downstream of vertical-tail leading edge, cm

α angle of attack, deg

β thrust deflection angle of second panel on wedge reverser with respect to nozzle reference line (fig. 10), deg

θ thrust deflection angle of first panel on wedge reverser with respect to nozzle reference line (fig. 10), deg

ϕ thrust deflection angle of third panel on wedge reverser with respect to nozzle reference line (fig. 10), deg

ψ angle of yaw (positive nose right), deg

Abbreviations:

BL butt line, cm

C-D convergent-divergent

FS fuselage station, cm

MAC mean aerodynamic chord

R/H right hand (looking upstream)

2-D two dimensional (nonaxisymmetric)

MODELS AND SUPPORT SYSTEMS

F-18 Model

Model.- A 0.10-scale F-18 afterbody jet-effects model (ref. 13) was employed for this investigation and is shown in the sketch of figure 1 and in the photograph of figure 2. The F-18 airplane is a light weight, highly maneuverable fighter with a relatively clean afterbody for nozzle installation. As shown by figures 1 and 2, the configuration is characterized by a straight wing with leading-edge strakes, inlet diverter bleed slots through the wing, twin vertical tails located well forward on the afterbody and close-spaced twin engines. The 0.10-scale model reproduced F-18 airplane lines except for faired-over inlets (required for powered-model tests and located on the forebody well forward of the afterbody) and wing alterations required for the model support system. The term "afterbody" as used in this paper refers to the metric portion of the model on which forces and moments are measured. The metric break, or seal station, begins at FS 144.78 and includes the aft fuselage, 2-D nozzles (including internal thrust hardware), and empennage surfaces. The model forebody and wing were

nonmetric. A 0.064-cm gap in the external skin at the metric-break station prevented fouling between the nonmetric forebody/wing and metric afterbody. A flexible rubber strip located in the metric-break gap was used as a seal to prevent internal flow in the model. The metric afterbody was attached to a six-component strain-gage balance which was grounded to the nonmetric forebody. The vertical tails were instrumented with static pressure orifices as indicated in figure 3.

Support system.- As shown in figures 1 and 2, the F-18 model was supported at the wing tips in the tunnel. The model fuselage reference plane was located 7.13 cm below the tunnel center line. The outer wing panels, from 65 percent of the semispan to the tip, were modified from airplane lines to accommodate the wing-tip support system and air supply system. The wing-tip booms were attached to the normal tunnel support system with V-struts as shown in figure 2. High-pressure air and instrumentation lines were routed through the V-struts and wing-tip booms entering the model fuselage through gun-drilled passages in both wings. The high-pressure air was dumped into a common high-pressure air plenum contained in the center section of the model.

Propulsion simulation system.- An external high-pressure air system provided a continuous flow of clean, dry air at a controlled temperature of about 294 K at the nozzles. This high-pressure air is transferred from a common high-pressure plenum in the model center section into the metric portion of the model by means of two flow-transfer assemblies. These flow-transfer devices have been used in several previous investigations (refs. 9, 10, 11, and 13) and are described in reference 9.

Transition (round to rectangular cross section) and instrumentation sections, including 17.9-percent-open choke plates, were attached to each of the flow-transfer assemblies and terminated at FS 169.32, which was the common connect station for all nozzles.

Two-dimensional convergent-divergent nozzle.- The 2-D C-D nozzles installed on the F-18 model are shown in the photographs of figures 4 and 5.

The 2-D C-D nozzle is a variable-area internal-expansion exhaust system which is a three-flap design between fixed sidewalls. The 2-D convergent flap controls nozzle-throat area. The 2-D variable-position divergent-flap and external-boattail-flap assembly controls both nozzle-exit area and thrust vector angle independently of throat area.

Thrust reversing is provided by a two-dimensional clamshell blocker and outer door combination. The reverser is located immediately downstream of the transition section that changes the exhaust duct from a round to a rectangular cross section. A photograph showing the 2-D C-D reverser installed on the model is shown in figure 6, and a sketch giving important reverser dimensions is presented in figure 7. Reverser exit ports are located on top and bottom of each nozzle (see fig. 6) 1.43 vertical-tail root-chord lengths downstream of the tail root-chord leading edge. This reverser was designed for 30-percent reverse thrust at 100-percent deployment. Installed reverser performance data for this design are presented in reference 13.

Wedge nozzle.- Figure 8 presents a photograph of the wedge nozzle installed on the F-18 model. The wedge nozzle investigated is a 2-D, variable-area, internal/external expansion exhaust system. Results on a similar nozzle are reported in reference 9. The nozzle has a collapsing wedge centerbody and a fixed external nozzle flap or boattail. The wedge geometry for a flight nozzle can be varied by unique scissor-type linkages and hinges which allow nozzle-exit area and area ratio to be varied independently of the throat area (ref. 14).

Thrust reversing is obtained on the wedge nozzle by variable-geometry, three-segment flaps located in the upper and lower wedge surfaces. Figure 9 presents a photograph of the wedge nozzle thrust reverser, and figure 10 presents a sketch showing details of the reverser design. The wedge nozzle reverser flaps (see fig. 10) were located approximately 1.60 vertical-tail root-chord lengths downstream of the tail root-chord leading edge (approximately 5 cm farther aft than the 2-D C-D reverser exit ports). This reverser was designed for 50-percent reversed thrust at 100-percent deployment.

F-15 Model

Model.- The F-15 model used for this investigation was a 0.047-scale, fully metric jet-effects model of a three-surface configuration (canard, wing, and horizontal tails) with an afterbody adapted to allow integration of nonaxisymmetric nozzles. Aerodynamic characteristics of this F-15 three-surface configuration have been obtained from a sting-mounted, 0.047 percent aerodynamic model and are reported in reference 15. A sketch of the model is shown in figure 11. The F-15 three-surface configuration is characterized by boom-mounted twin vertical tails (2° toe out angle), horizontal tails located well aft on the afterbody, close-spaced twin engines, and forward mounted canards. For the current investigation the canards were set at a nominal angle of -6° (leading edge down).

Support system.- The F-15 model was supported in the tunnel by a sting-strut system as shown in figure 12. High-pressure air lines and all instrumentation were routed through the support system. An internal six-component strain-gage balance was mounted to the strut through an adapter which could be preset before each run at a selected model yaw angle.

Propulsion simulation system.- The external high-pressure air supply as described for the F-18 model was also used to simulate nozzle exhaust flow for the F-15 model. The air was transferred to the nozzles through twin flow-transfer assemblies similar in design to those used for the F-18 model. Figure 13 shows a sketch of the F-15 model flow-transfer system.

Transition (from round to rectangular cross section) and instrumentation sections were downstream of the 30-percent-open choke plates which were located in each exhaust flow tailpipe at FS 83.35. The transition section terminated at FS 91.24.

Two-dimensional convergent-divergent nozzle.- Figure 14 shows a photograph of the F-15 model with 2-D C-D nozzles installed. Figure 15 presents a photograph of the 2-D C-D nozzles installed with thrust reversers fully deployed.

This 2-D C-D nozzle design simulates a variable area, internal expansion flight nozzle with fixed sidewalls. Throat area and exit area are independently controlled on full-scale hardware by separate actuation of the convergent and divergent nozzle flaps. Thrust reversal is accomplished by rotary actuation of the convergent flaps (closing throat area) with the upstream end of the convergent flaps simultaneously opening reverse flow ports. A complete description of this nozzle mechanism is given in reference 10. The resulting reverse flow exit ports are located between the twin vertical tails at 58.5 percent of the vertical-tail root chord. Figure 16 presents a sketch of the model nozzle thrust reverser in the fully deployed position which was designed for approximately 50-percent thrust reversal.

APPARATUS AND METHODS

Wind Tunnel

The experimental investigations were conducted in the Langley 16-Foot Transonic Tunnel. This tunnel is a single-return, atmospheric tunnel with a slotted, octagonal test section and continuous air exchange. The wind tunnel has a variable airspeed up to a Mach number of 1.30. Test-section plenum suction is used for speeds above a Mach number of 1.10. A complete description of this facility and operating characteristics can be found in reference 16.

Instrumentation

F-18 model.- Flow conditions in each nozzle were determined from two total pressure rakes and one total temperature probe located in the instrumentation section aft of the transition section and choke plate (see Models and Support Systems section). Each rake, one from the top and one from the side of both instrumentation sections, contained three total pressure probes.

Both vertical tails of the F-18 model were instrumented with nine static-pressure orifices, each positioned as shown in the sketch of figure 3. The static pressure orifices on the left-hand (looking upstream) vertical tail were located on the inboard surface of the tail. On the right-hand vertical tail, the static pressure orifices were located on the outboard surface. All pressures were measured with individual pressure transducers.

F-15 model.- Nozzle flow conditions in each nozzle were determined from two total pressure probes, one from the top and one from the side, and one total temperature probe, all located in an instrumentation section aft of the choke plate and transition section. (See Models and Support Systems section.)

Forces and moments on the entire F-15 model were measured with a six-component strain-gage balance mounted in the model. All pressures were measured with individual pressure transducers.

Tests

All tests were conducted in the Langley 16-Foot Transonic Tunnel. Test conditions for both models are given in the following table:

Model	Nozzle	Cruise A_e/A_t	M	α, deg	ψ, deg	$p_{t,j}/p_\infty$
F-18	2-D C-D	1.15	0.6, 0.9, 1.2	-2 to 6	0	Jet off to 8.0
	Wedge	1.10	0.6, 0.9	-2 to 6	0	Jet off to 8.0
F-15	2-D C-D	1.20	0.6, 0.9	-2 to 15	0, 5, 10	Jet off, 3.5, 5.0

Reynolds number per meter varied from 1.12×10^7 to 1.31×10^7. Basic data were obtained by varying angle of attack at a set Mach number and nozzle pressure ratio.

All tests of the F-18 model were conducted with 0.25-cm-wide boundary-layer transition strips consisting of No. 100 silicon carbide grit sparsely distributed in a thin film of lacquer. These strips were located 3.81 cm from the tip of the nose and 2.54 cm aft (streamwise) of all lifting and inlet (imaginary) leading edges.

All tests of the F-15 model were conducted with 0.25-cm-wide boundary-layer transition strips consisting of No. 120 carborundum grit. These strips were located 1.91 cm aft of the nose and the inlet fairings. Transition strips on all lifting surfaces were located at 5 percent local chord.

In order to obtain the effect of thrust reverser operation on vertical-tail loads on the F-15 model (see Data Reduction section), it was tested with both vertical tails off and with the right-hand vertical tail installed (left-hand vertical tail off).

Data Reduction

All data for both the model and the wind tunnel were recorded simultaneously on magnetic tape. Approximately 50 frames of data, taken at a rate of 10 frames per second, were recorded for each data point; average values were used in computations. Corrections were made to the force data for both models to account for bellows/balance interaction tares (refs. 9 and 13). The recorded data were used to compute standard force and moment coefficients using wing area, mean geometric chord, and span for reference area and lengths. A flow angularity adjustment of 0.1°, which is the average angle measured in the Langley 16-Foot Transonic Tunnel, was also applied for both models.

F-18 model.- Differential pressure coefficients on the F-18 vertical tail were obtained by subtracting inboard vertical-tail pressures from outboard vertical-tail pressures. Side-force coefficient of the vertical tail was computed from the differential pressures and an area assigned to each differential pressure.

F-15 model.- Vertical-tail side-force coefficient on the F-15 model during reverse thrust operation was computed from the model total yawing moment. With the right-hand vertical tail only installed (left-hand vertical tail off), it was assumed that the yawing moment developed by the model (symmetrical about pitch plane except for vertical tail) resulted from a side force on the single (right-hand) installed vertical tail. An estimate of the vertical-tail side force was then calculated by dividing total model yawing moment by the vertical-tail moment arm (measured from the vertical-tail MAC to model moment reference center).

RESULTS AND DISCUSSION

F-18 Model

The effects of thrust reverser operation on the F-18 model vertical-tail pressures and loads with both the 2-D C-D and wedge nozzles are presented in figures 17 to 21. Figures 17 and 18 show typical measured pressure distributions on the vertical tails. Incremental pressure coefficients are given in figures 19 and 20 and the integrated tail side-force coefficients are shown in figure 21.

Typical jet-off pressure distributions (fig. 17) indicate a channeling effect of the vertical tails; that is, the local velocities on the inboard side of the vertical tails are higher (lower pressure coefficients) at subsonic speeds (figs. 17(a) and 17(b)) and lower at supersonic speeds (fig. 17(c)) than the local velocities on the outboard side of the vertical-tail surfaces. The influence of thrust reverser operation (jet on) on vertical-tail pressure distributions obtained at $M = 0.6$ and 0.9 is extensive, as shown by the increased pressure coefficients (less negative) over the entire ($x/c = 0.25$ to 0.75 and row 1 to row 3) inboard and outboard surfaces of the vertical tail. This increase in pressure coefficient indicates a reduction in local velocities around the vertical tails which is probably caused by reverse flow plume blockage of the external free-stream flow or by immersion of the tail in the reverse flow. At $M = 1.2$, thrust reverser operation had little or no effect on vertical-tail pressure distribution (fig. 17(c)). At supersonic speeds, since downstream pressure disturbances can only feed upstream through the boundary layer, the free-stream dynamic pressure is apparently sufficient to turn the reverse flow plume back downstream to such an extent that no reverse flow washed the vertical tails except for the aft most ($x/c = 0.75$) outboard location near the vertical-tail tip (row 1).

A comparison of pressure distributions during thrust reverser operation for the 2-D C-D nozzle (designed for 30-percent reverse static thrust) and the wedge

nozzle (designed for 50-percent reverse static thrust) is shown in figure 18. Both nozzle reverser designs show similar trends on vertical-tail pressure distributions even though they were designed to produce substantially different levels of reverse thrust. It is believed that the differences in pressure-coefficient magnitude for the two reverser designs shown in figure 18 are caused by reverser location with respect to the vertical tails (wedge reverser approximately 5 cm farther downstream than 2-D C-D reverser) rather than the different levels of design reverse thrust.

The effect of thrust reversing on vertical-tail loads is best seen by examining the integrated vertical-tail side-force coefficients $C_{Y,tail}$ of figure 21 (data from figs. 19 and 20 times assigned incremental areas) for the model with both the 2-D C-D and the wedge 100-percent deployed reverser nozzles installed. The jet-off (lowest nozzle pressure ratio tested at each Mach number) vertical-tail side-force coefficient is always a positive or inward force at subsonic speeds. Since the vertical tails of the F-18 are mounted well forward of the nozzle exit, it is believed that the jet-off vertical-tail loads shown in figure 21 are probably indicative of the power-on vertical-tail loads with the nozzles operating in a cruise or nonreverse mode. At $M = 0.6$ and $M = 0.9$, as nozzle pressure ratio increases, there is an unloading of the vertical tail such that the vertical-tail side-force coefficient eventually becomes negative. Negative values of $C_{Y,tail}$ indicate outward forces on the vertical tails. Although tail side-force coefficient increases with increasing angle of attack, the increment in tail side force from jet-off to maximum nozzle pressure ratio (effect of reverser operation) remains nearly constant for the angle-of-attack range tested. Although the wedge nozzle reverser was designed to produce substantially higher levels of static reverse thrust than the 2-D C-D reverser (50 percent as compared to 30 percent), the effects of wedge nozzle reverser operation (jet off to jet on) on vertical-tail side-force coefficient are somewhat less than observed for the 2-D C-D reverser (compare figs. 21(a) and 21(b)), probably because the wedge nozzle reverser flaps are located farther aft of the vertical tails than the reverser ports of the 2-D C-D nozzle. (Compare figs. 7 and 10.) At $M = 1.2$, 2-D C-D nozzle reverser operation had no effect on vertical-tail side-force coefficient (fig. 21(a)). This result was expected from examination of the pressure distributions shown in figure 17(c) and indicates that, for configurations similar to the F-18 (vertical tails well forward), in-flight thrust reversing at supersonic speeds does not affect vertical-tail loads. It is interesting to note that the largest inward force on the vertical tails occurred at a jet-off condition ($M = 0.9$; $\alpha = 6.1^{\circ}$) which, as discussed previously, is representative of a nonreverse or cruise nozzle operating condition and that the largest outward force on the vertical tails occurred at $M = 1.2$, and $\alpha = 0.1^{\circ}$ where tail load was independent of reverser operation. Thus, over the range of test conditions investigated, addition of an in-flight reverser to the F-18 configuration would have no impact on the design side-force loads of the vertical tails. Although a forward placement of the vertical tails, as on the F-18, removes them from most adverse loads as a result of thrust reversal, it also exposes the horizontal tails to a possible direct influence of thrust reverser operation. Reference 13 indicates that thrust reverser operation does cause a loss in F-18 horizontal-tail effectiveness.

F-15 Model

An estimate of vertical-tail loads for the F-15 model was made by using the measured lateral aerodynamic data for the entire model with one vertical tail and no vertical tails installed (see Data Reduction section). Using these data, two different methods were employed to obtain a vertical-tail side-force coefficient.

The first, and probably most accurate method, was to calculate an incremental side-force coefficient by subtracting the total side-force coefficient for the model with both vertical tails removed from the total side-force coefficient for the model with only the right-hand vertical tail installed. A positive total or incremental side-force coefficient indicates an outward force (higher pressure on inboard side of vertical tail than on outboard side) on the right-hand vertical tail. The total side-force coefficient for the configuration with only one vertical tail is presented in figure 22, and the resulting incremental side-force coefficient (positive ΔC_Y indicates outward force on vertical tails) is shown in figure 23 as a function of angle of attack and nozzle pressure ratio at Mach numbers of 0.6 and 0.9. Data were obtained at jet-off and typical operating nozzle pressure ratios at each Mach number only.

By comparing the change in vertical-tail side-force coefficient from jet-off to jet-on conditions in figures 21 and 23, it is readily apparent that the F-15 vertical-tail loads are much greater in magnitude than those measured on the F-18. The effect of thrust reverser operation on incremental side-force coefficient (approximation of tail load) shows no indication of diminishing on the F-15 configuration from Mach number 0.6 to 0.9. The greater sensitivity of the F-15 configuration to reverser operation probably results from the closer proximity of the vertical tails to the reverser exhaust ports for this configuration. (Compare figs. 1 and 11.)

The second method of obtaining vertical-tail side-force coefficient assumes that all yawing moment measured on the model is due to a side force on the vertical tail. These tail load data are presented in figure 24. Comparing the vertical-tail side force calculated in this manner (see fig. 24) with the incremental side-force coefficient value at 0° sideslip (fig. 23) shows that the values calculated from yaw are slightly higher.

For analysis of the F-15 data, it is important to emphasize that the values of vertical-tail side-force coefficient presented are only estimates and not true loads data. In addition, the external flow field over the afterbody of the F-15 model is probably altered by the removal of one vertical tail. However, these data do indicate a potential problem with vertical-tail design for loads during thrust reverser operation and also a potential loss in rudder effectiveness when the vertical tails are in close proximity to reverser exhaust ports.

CONCLUDING REMARKS

Investigations were conducted in the Langley 16-Foot Transonic Tunnel to provide data on the effect of simulated in-flight thrust reversing on

vertical-tail loads of a 0.10-scale model of the prototype F-18 airplane and a 0.047-scale model of the F-15 three-surface configuration. Test data were obtained at static conditions and at Mach numbers from 0.6 to 1.2 over an angle-of-attack range from -2° to 15°. Nozzle pressure ratio was varied from jet off to about 8.0.

Results from these investigations indicate that the use of an in-flight thrust reverser with twin-vertical-tail configurations at subsonic Mach numbers increases the inboard vertical-tail pressures and thus tends to produce an outward side force on the vertical tails, depending on nozzle pressure ratio, angle of attack, and Mach number. The magnitude of the vertical-tail side force resulting from reverser operation is thought to be dependent upon the location of the vertical tails with respect to the reverser exit ports. Results from the F-18 model indicate that larger effects on vertical-tail side-force coefficient were obtained with a two-dimensional convergent-divergent (2-D C-D) nozzle reverser than with a wedge nozzle reverser which was located approximately 5 cm aft of the 2-D C-D reverser location; this result occurred even though the wedge nozzle reverser was designed to provide substantially higher levels of static reverse thrust than the 2-D C-D nozzle reverser (50 percent compared to 30 percent). Estimated vertical-tail side-force loads on the F-15, which had a 2-D C-D nozzle reverser with exit ports located between the twin vertical tails, were much greater in magnitude than those measured on the F-18 with reverser ports or flaps located aft of the vertical tails.

On the F-18 model, the largest inward and outward forces measured on the twin vertical tails resulted from aerodynamic loads rather than reverser operation induced loads. Thus, for the test range of this investigation, addition of an in-flight reverser to the F-18 configuration would have no impact on the design side-force loads of the vertical tails.

Langley Research Center
National Aeronautics and Space Administration
Hampton, VA 23665
June 30, 1981

REFERENCES

1. Martens, Richard E.: F-15 Nozzle/Afterbody Integration. J. Aircr., vol. 13, no. 5, May 1976, pp. 327-333.

2. Hiley, P. E.; Wallace, H. W.; and Booz, D. E.: Nonaxisymmetric Nozzles Installed in Advanced Fighter Aircraft. J. Aircr., vol. 13, no. 12, Dec. 1976, pp. 1000-1006.

3. Berrier, Bobby L.; Palcza, J. Lawrence; and Richey, G. Keith: Nonaxisymmetric Nozzle Technology Program - An Overview. AIAA Paper 77-1225, Aug. 1977.

4. Capone, Francis J.: The Nonaxisymmetric Nozzle - It is for Real. AIAA Paper 79-1810, Aug. 1979.

5. Miller, Eugene H.; and Protopapas, John: Nozzle Design and Integration in an Advanced Supersonic Fighter. AIAA Paper 79-1813, Aug. 1979.

6. Stevens, H. L.: F-15/Nonaxisymmetric Nozzle System Integration Study Support Program. NASA CR-135252, 1978.

7. F-15 2-D Nozzle System Integration Study. Volume I - Technical Report. NASA CR-145295, 1978.

8. Gowadia, N. S.; Bard, W. D.; and Wooten, W. H.: YF-17/ADEN System Study. NASA CR-144882, 1979.

9. Capone, Francis J.; and Maiden, Donald L.: Performance of Twin Two-Dimensional Wedge Nozzles Including Thrust Vectoring and Reversing Effects at Speeds up to Mach 2.20. NASA TN D-8449, 1977.

10. Capone, Francis J.: Static Performance of Five Twin-Engine Nonaxisymmetric Nozzles With Vectoring and Reversing Capability. NASA TP-1224, 1978.

11. Hiley, P. E.; Kitzmiller, D. E.; and Willard, C. M.: Installed Performance of Vectoring/Reversing Nonaxisymmetric Nozzles. J. Aircr., vol. 16, no. 8, Aug. 1979, pp. 532-538.

12. Pendergraft, O. C.: Comparison of Axisymmetric and Nonaxisymmetric Nozzles Installed on the F-15 Configuration. AIAA Paper 77-842, July 1977.

13. Capone, Francis J.; and Berrier, Bobby L.: Investigation of Axisymmetric and Nonaxisymmetric Nozzles Installed on a 0.10-Scale F-18 Prototype Airplane Model. NASA TP-1638, 1980.

14. Goetz, Gerald F.; Young, John H.; and Palcza, J. Lawrence: A Two-Dimensional Airframe Integrated Nozzle Design With Inflight Thrust Vectoring and Reversing Capabilities for Advanced Fighter Aircraft. AIAA Paper No. 76-626, July 1976.

15. Henderson, William P.; and Leavitt, Laurence D.: Stability and Control Characteristics of a Three Surface Configuration at Angles of Attack up to 45°. NASA TM-83171, 1981.

16. Corson, Blake W., Jr.; Runckel, Jack F.; and Igoe, William B.: Calibration of the Langley 16-Foot Transonic Tunnel With Test Section Air Removal. NASA TR R-423, 1974.

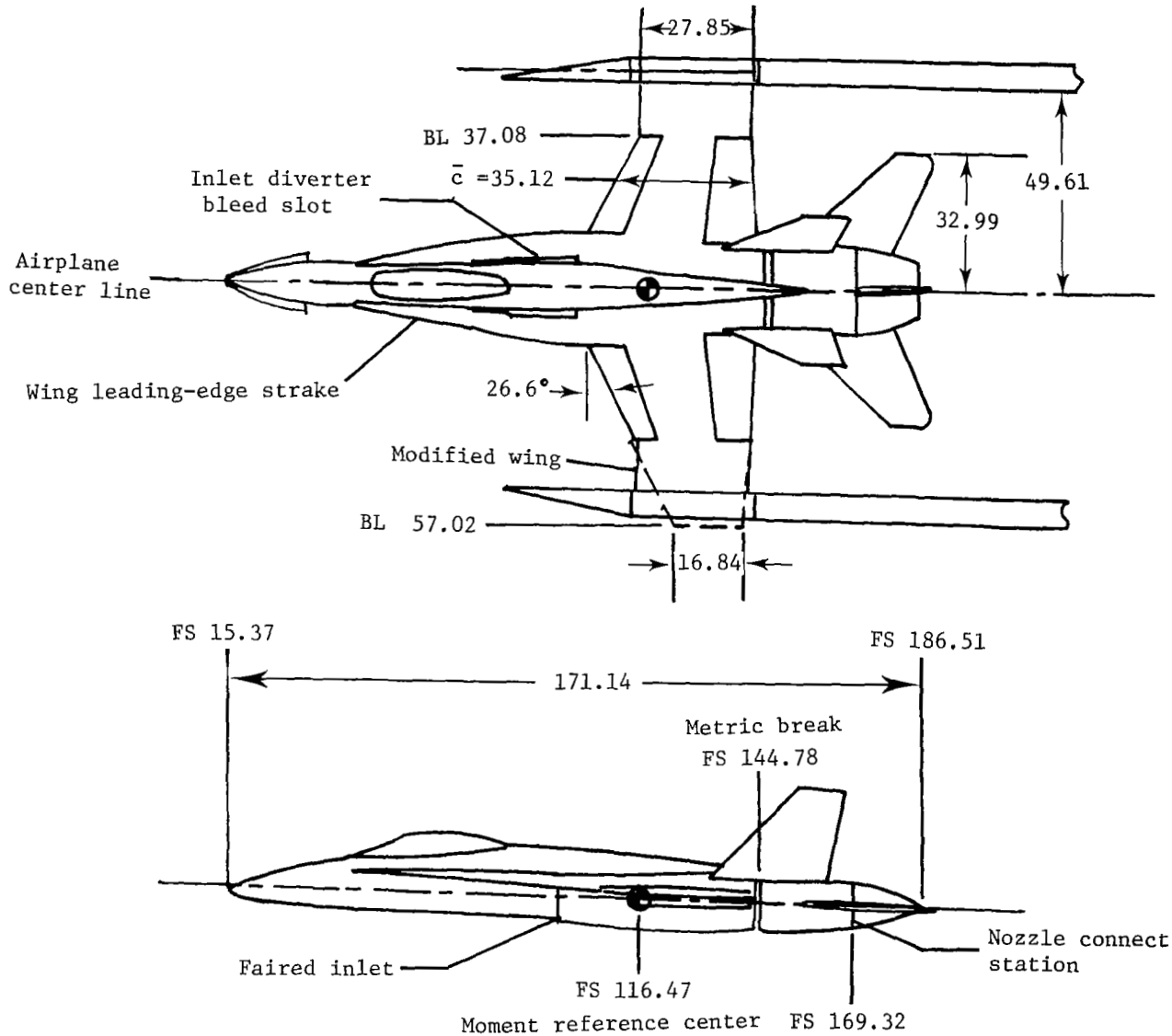

Figure 1.- Sketch of F-18 model. All dimensions are in centimeters unless otherwise specified.

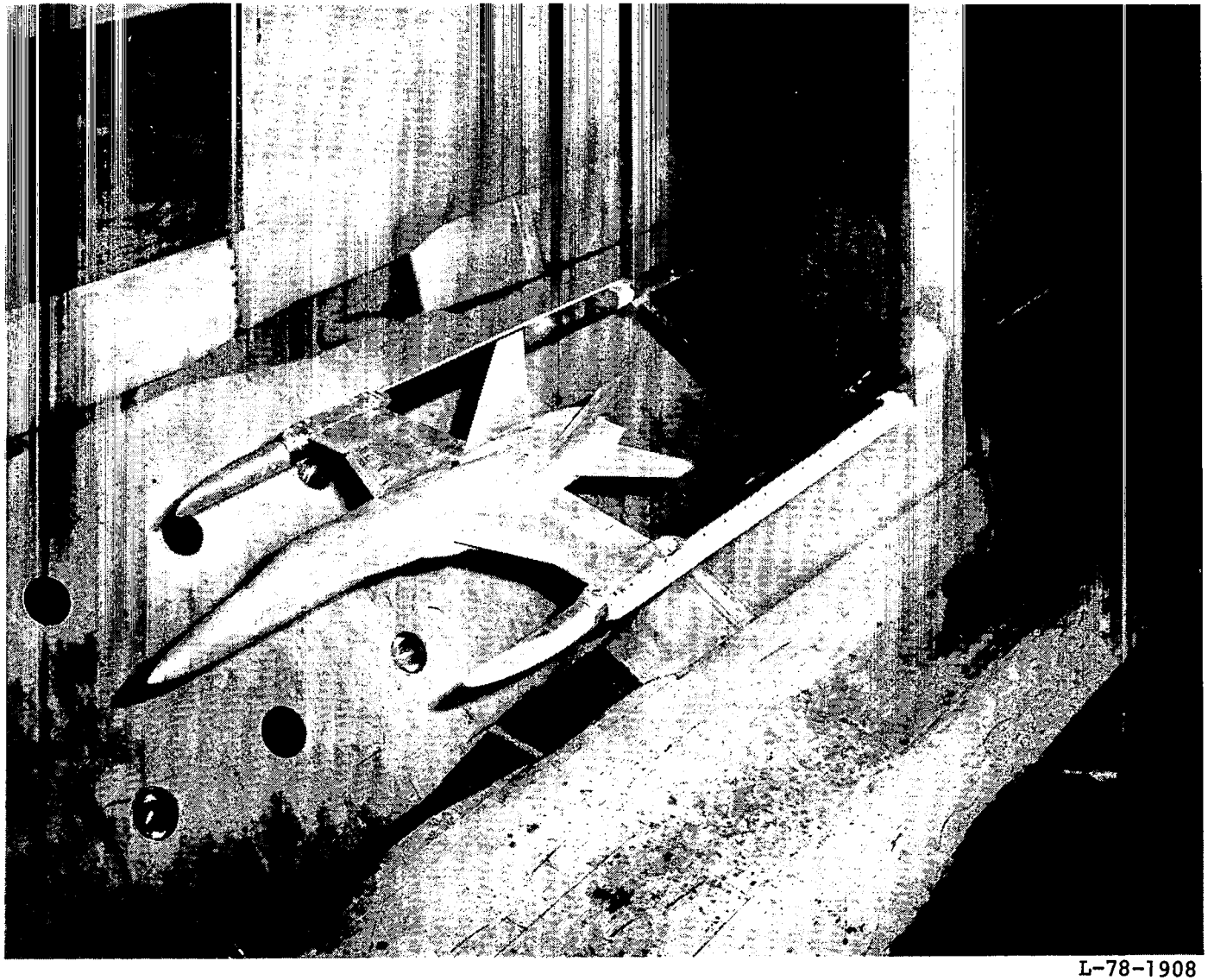

L-78-1908

Figure 2.- Photograph showing installation of F-18 model in Langley 16-Foot Transonic Tunnel.

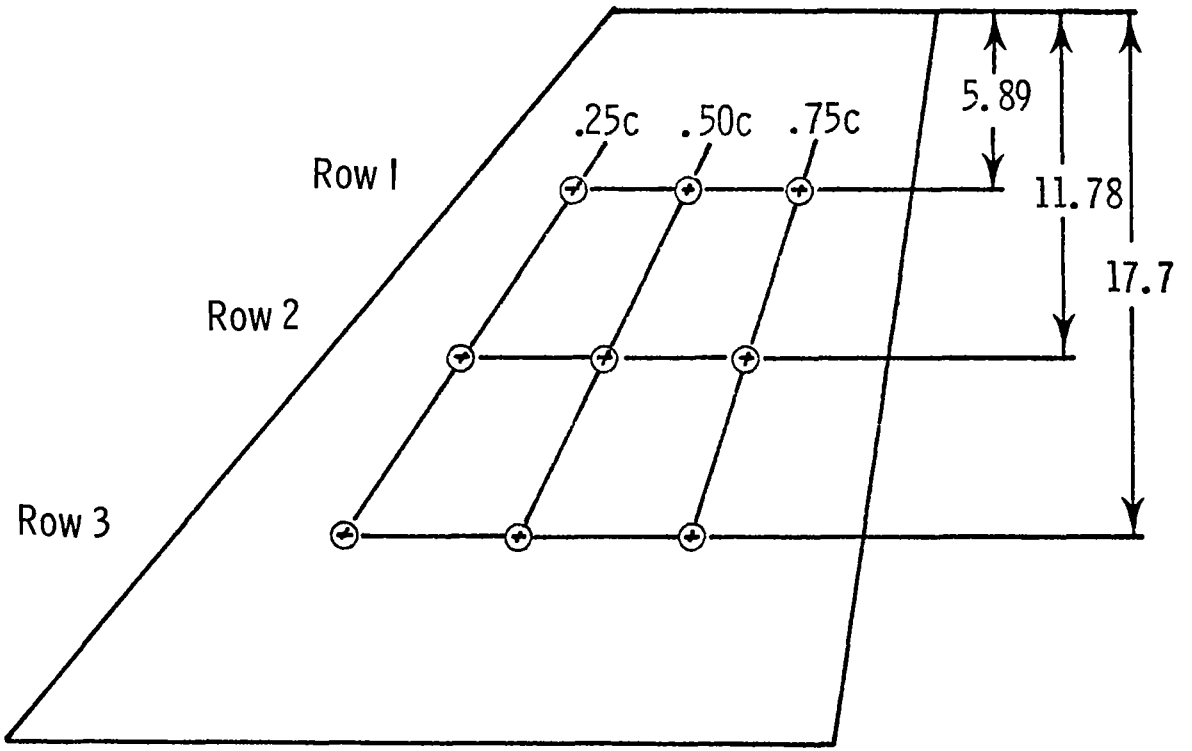

Figure 3.- Position of pressure taps on F-18 vertical tail. All dimensions are in centimeters unless otherwise specified.

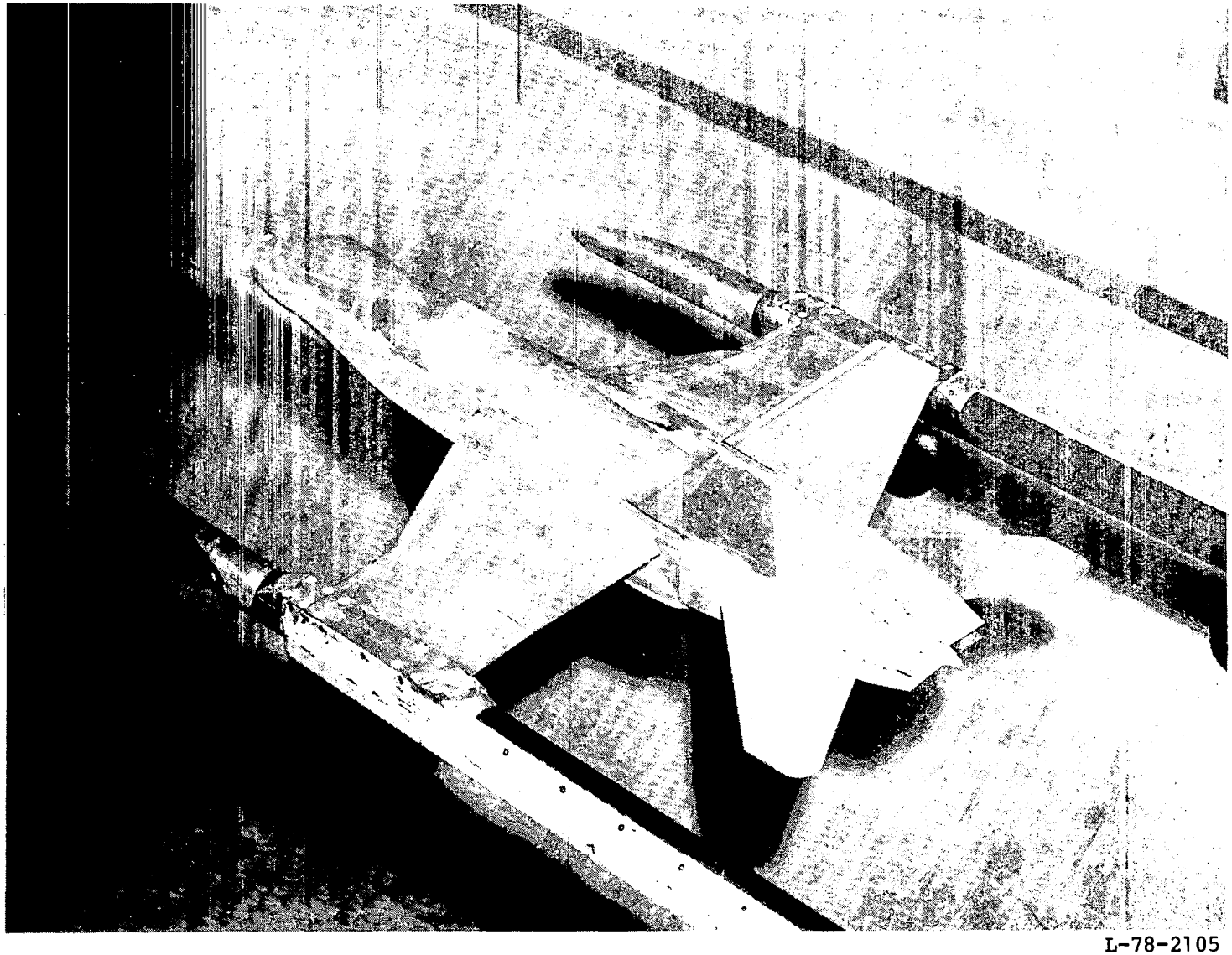

L-78-2105

Figure 4.- Overall view of 2-D C-D nozzle installed on F-18 model.

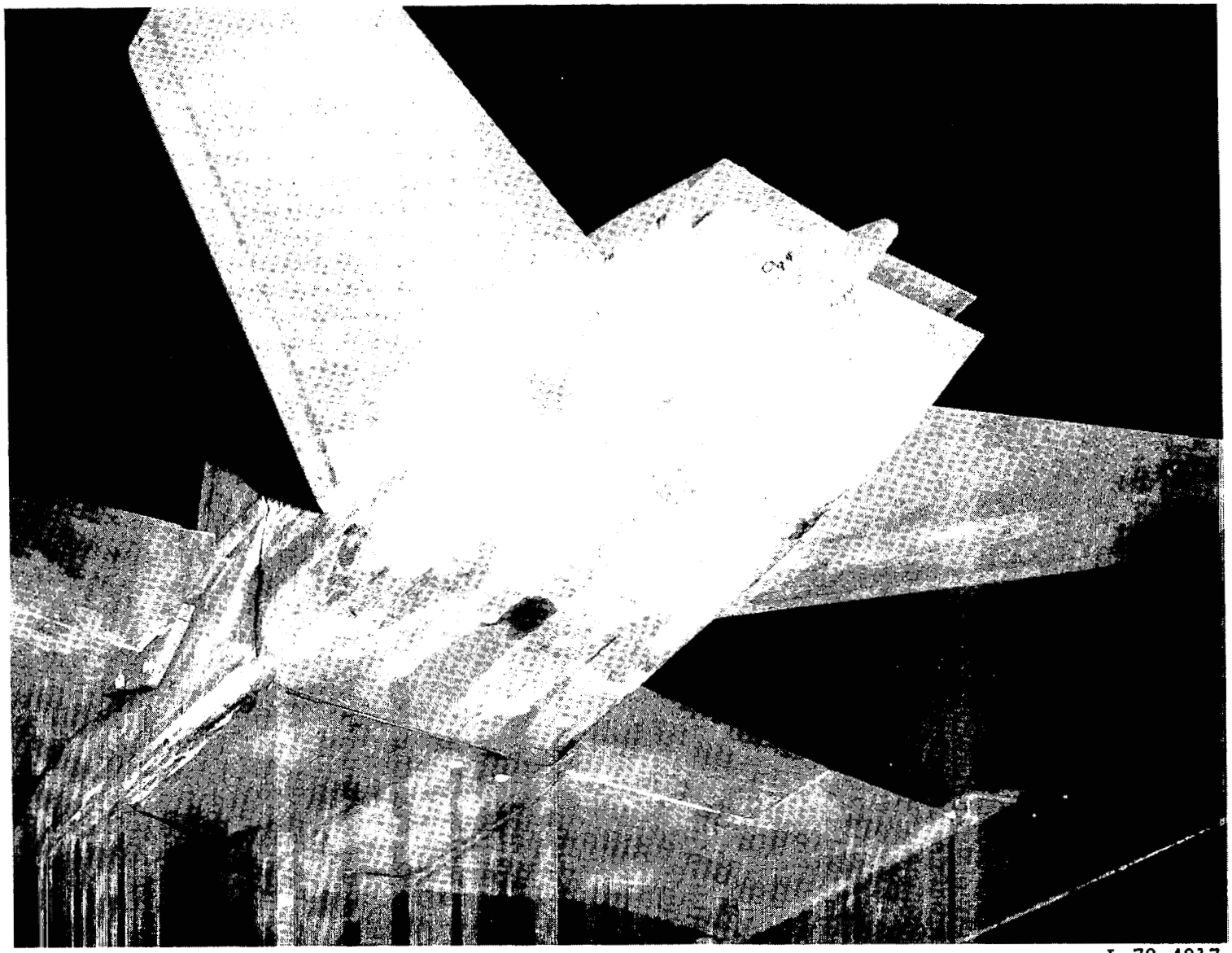

L-78-4817

Figure 5.- Photograph showing 2-D C-D nozzle, dry power, installed on F-18 model.

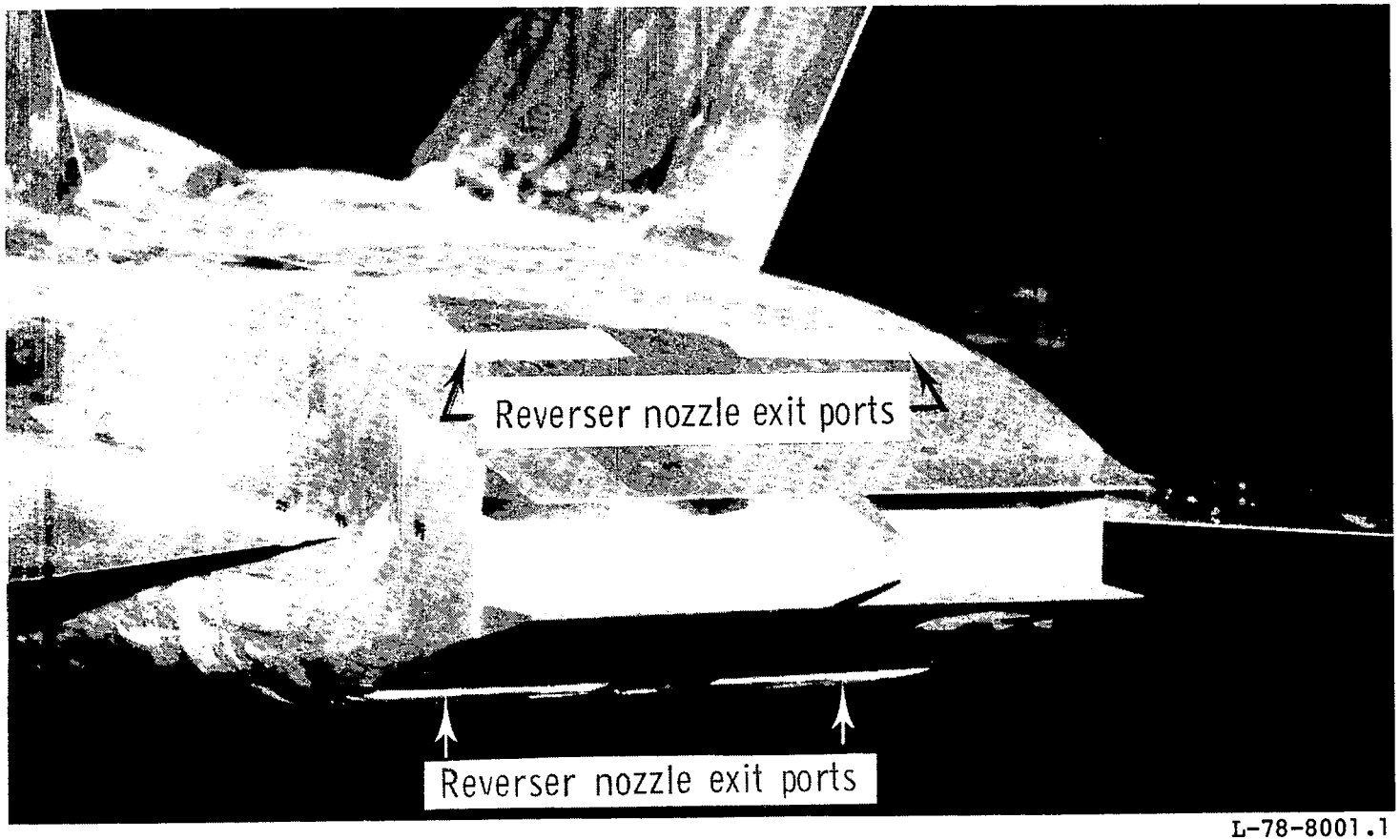

L-78-8001.1

Figure 6.- Photograph showing fully deployed 2-D C-D thrust reverser on F-18 model.

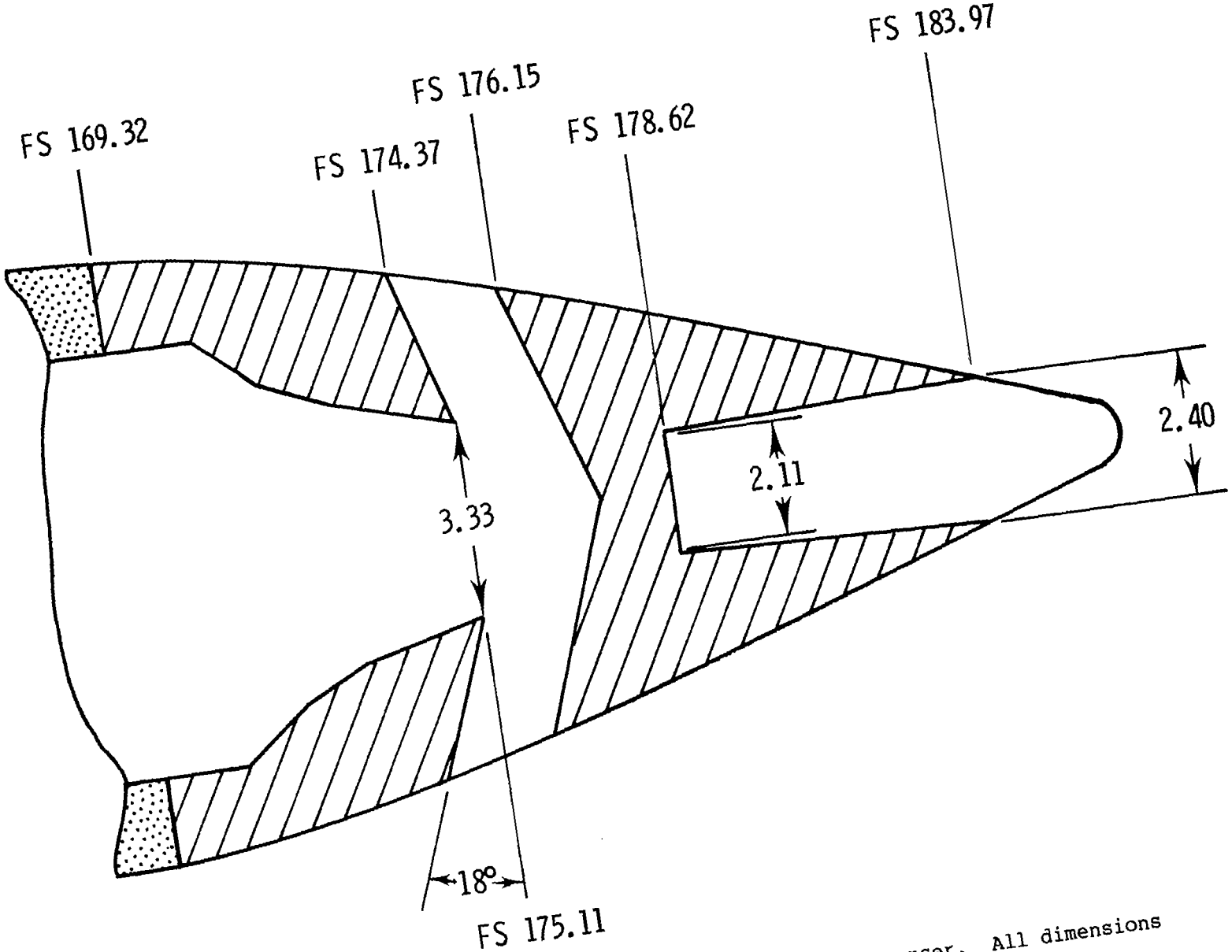

s fully deployed 2-D C-D thrust reverser. All dimensions
nless otherwise specified.

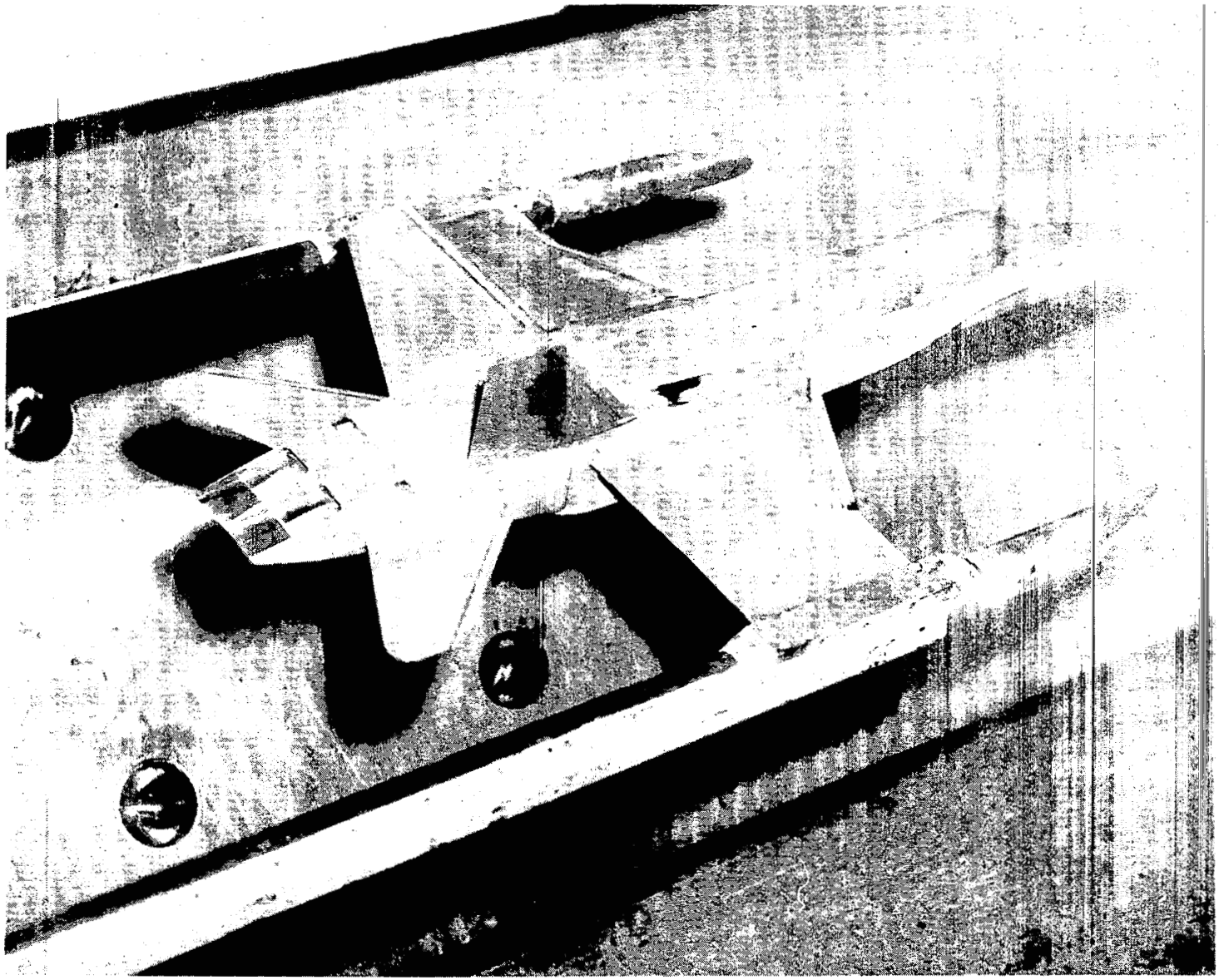

L-78-2555

Figure 8.- Overall view of wedge nozzle installed on F-18 model.

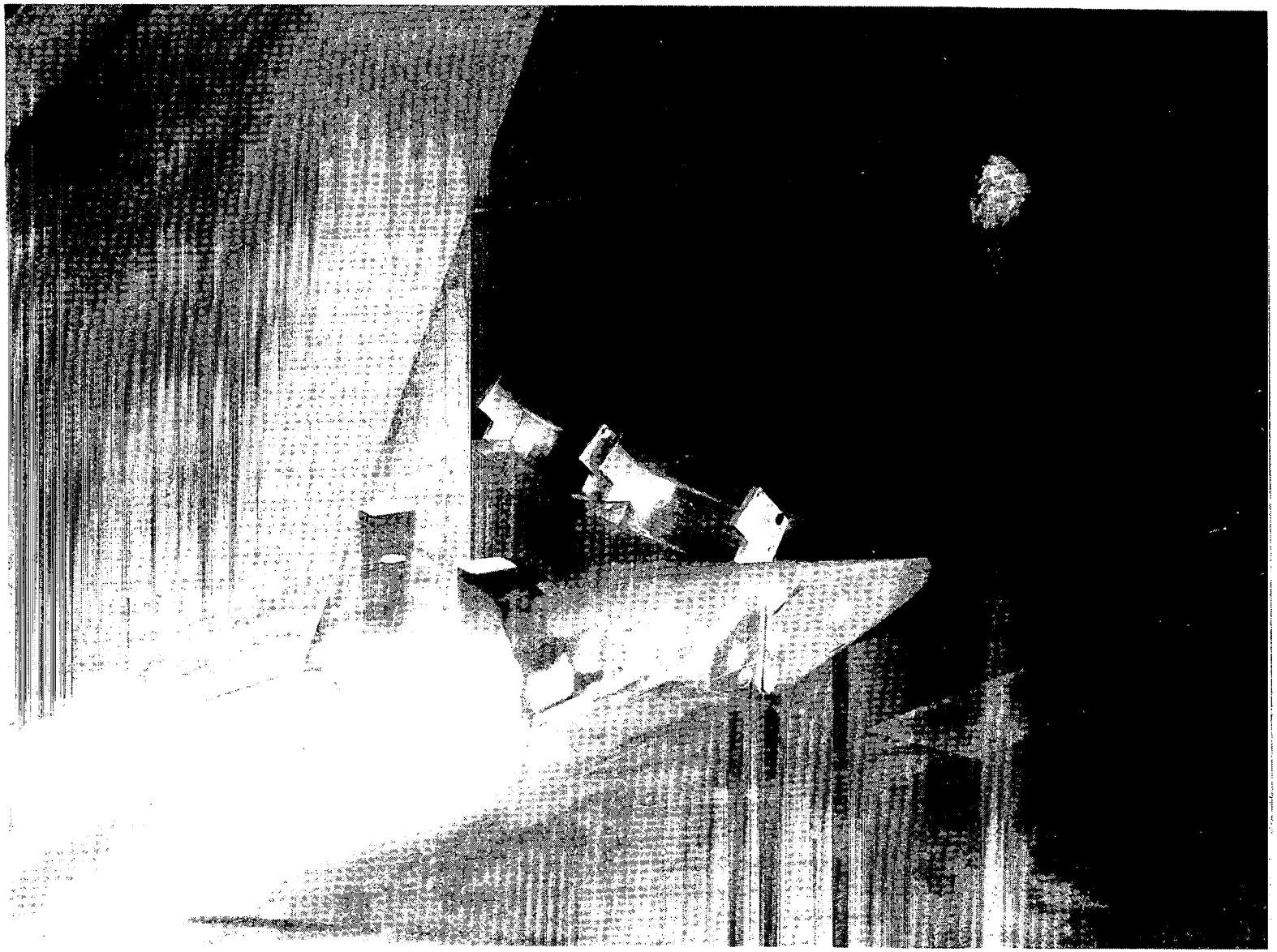

L-81-167

Figure 9.- Photograph showing fully deployed wedge nozzle thrust reverser on F-18 model.

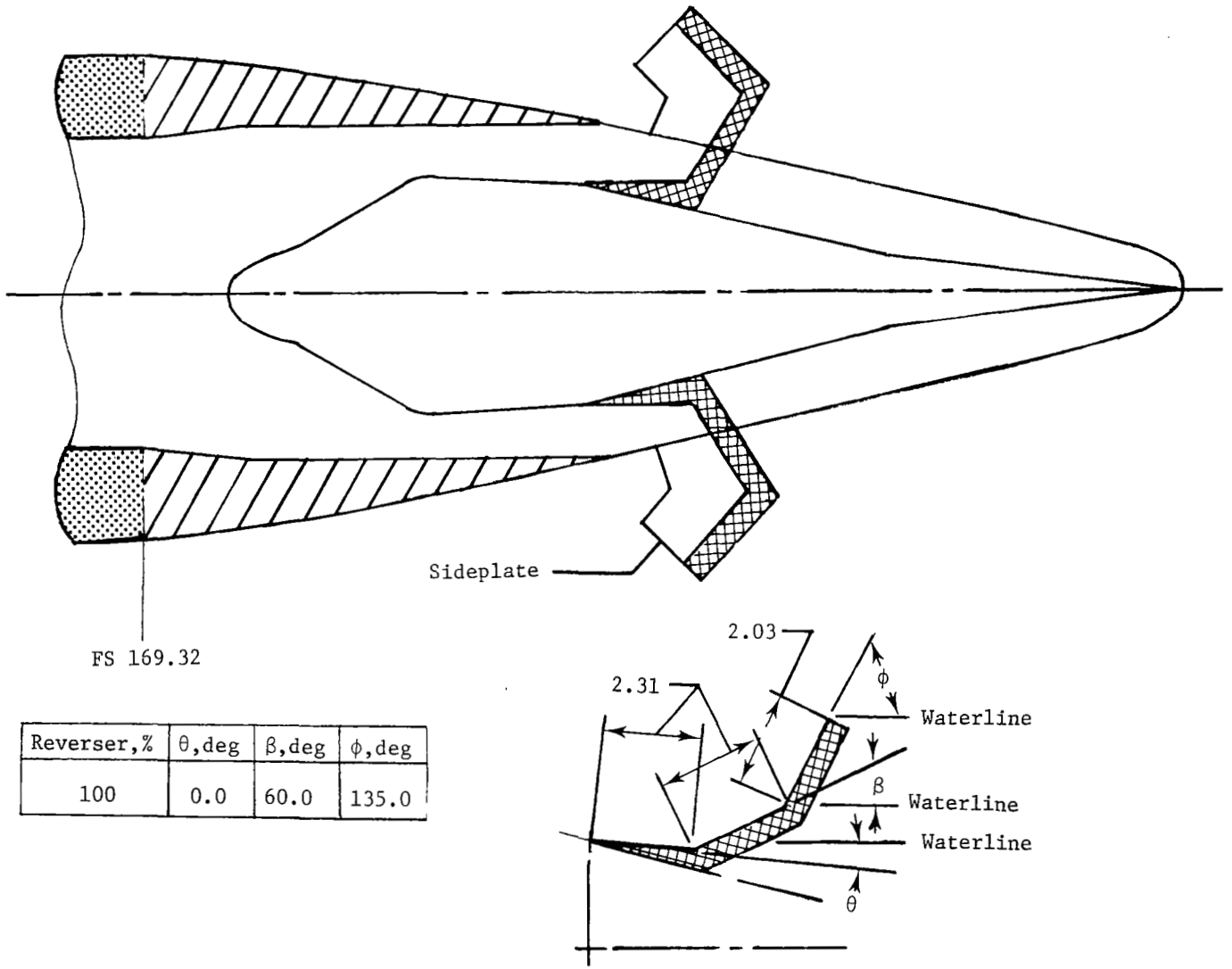

Reverser,%	θ,deg	β,deg	ϕ,deg
100	0.0	60.0	135.0

Figure 10.- Sketch showing fully deployed thrust reverser on wedge nozzle. All dimensions are in centimeters unless otherwise specified.

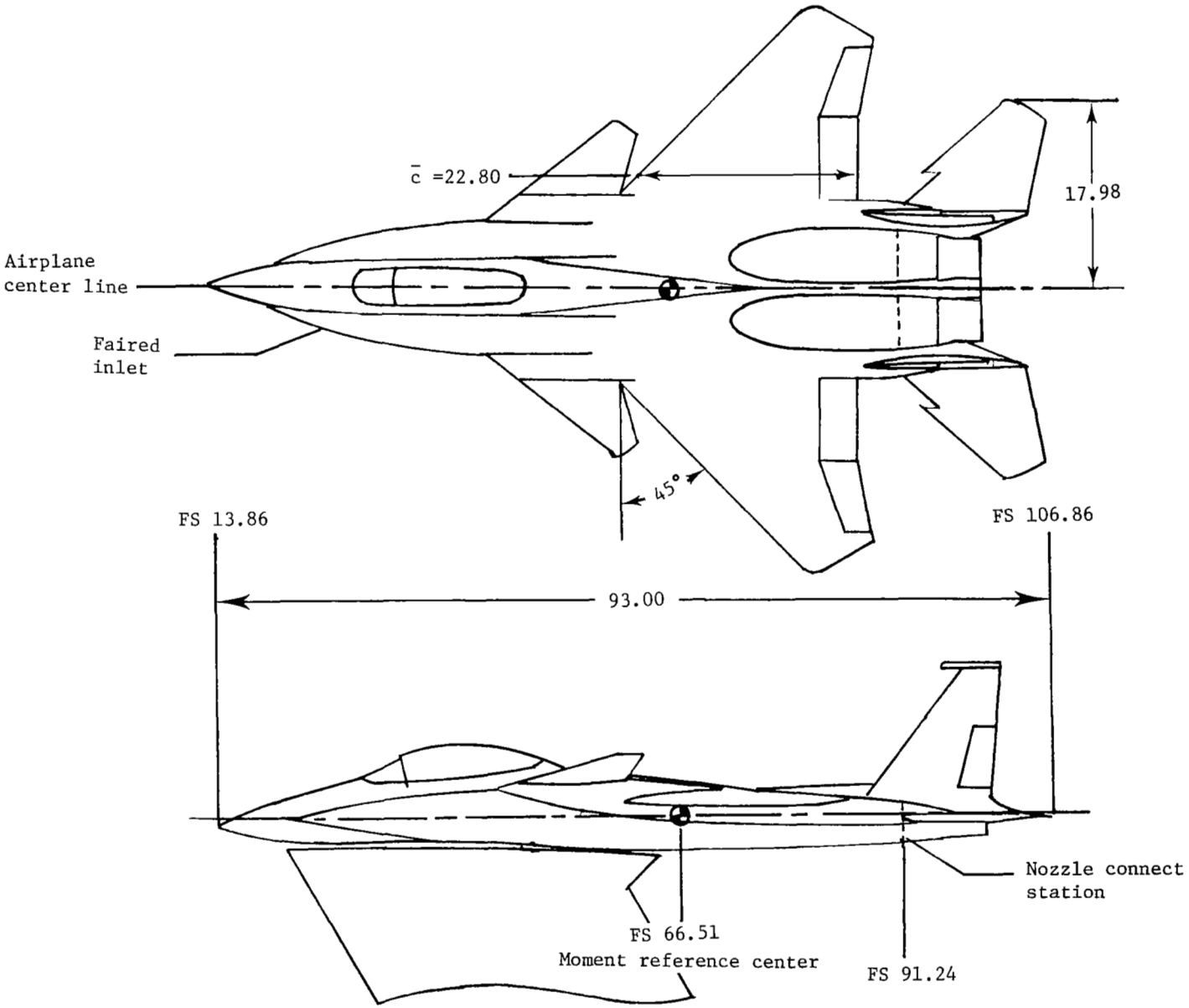

Figure 11.- Sketch of F-15 three-surface configuration. All dimensions are in centimeters unless otherwise specified.

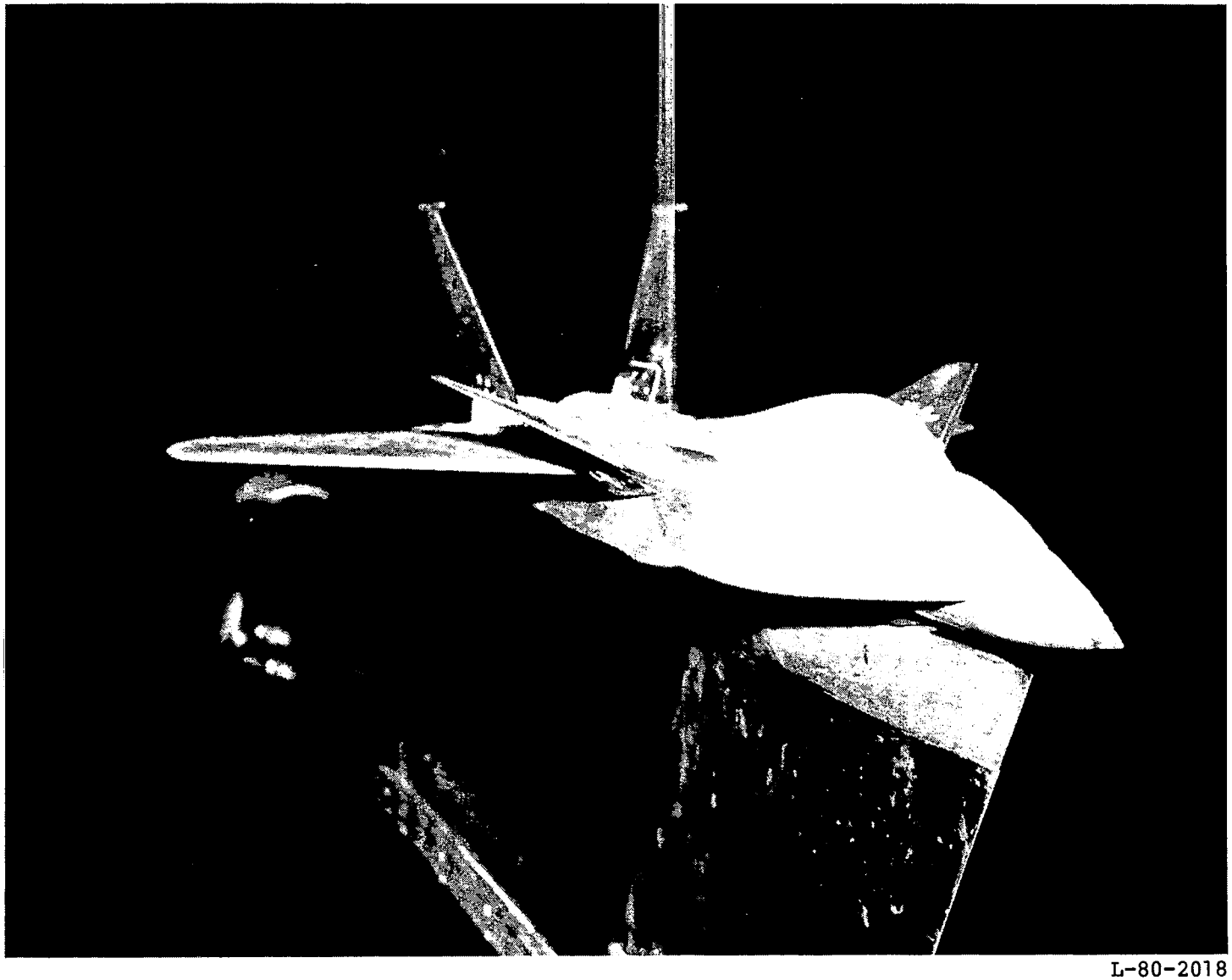

L-80-2018

Figure 12.- Photograph showing installation of F-15 three-surface configuration in Langley 16-Foot Transonic Tunnel.

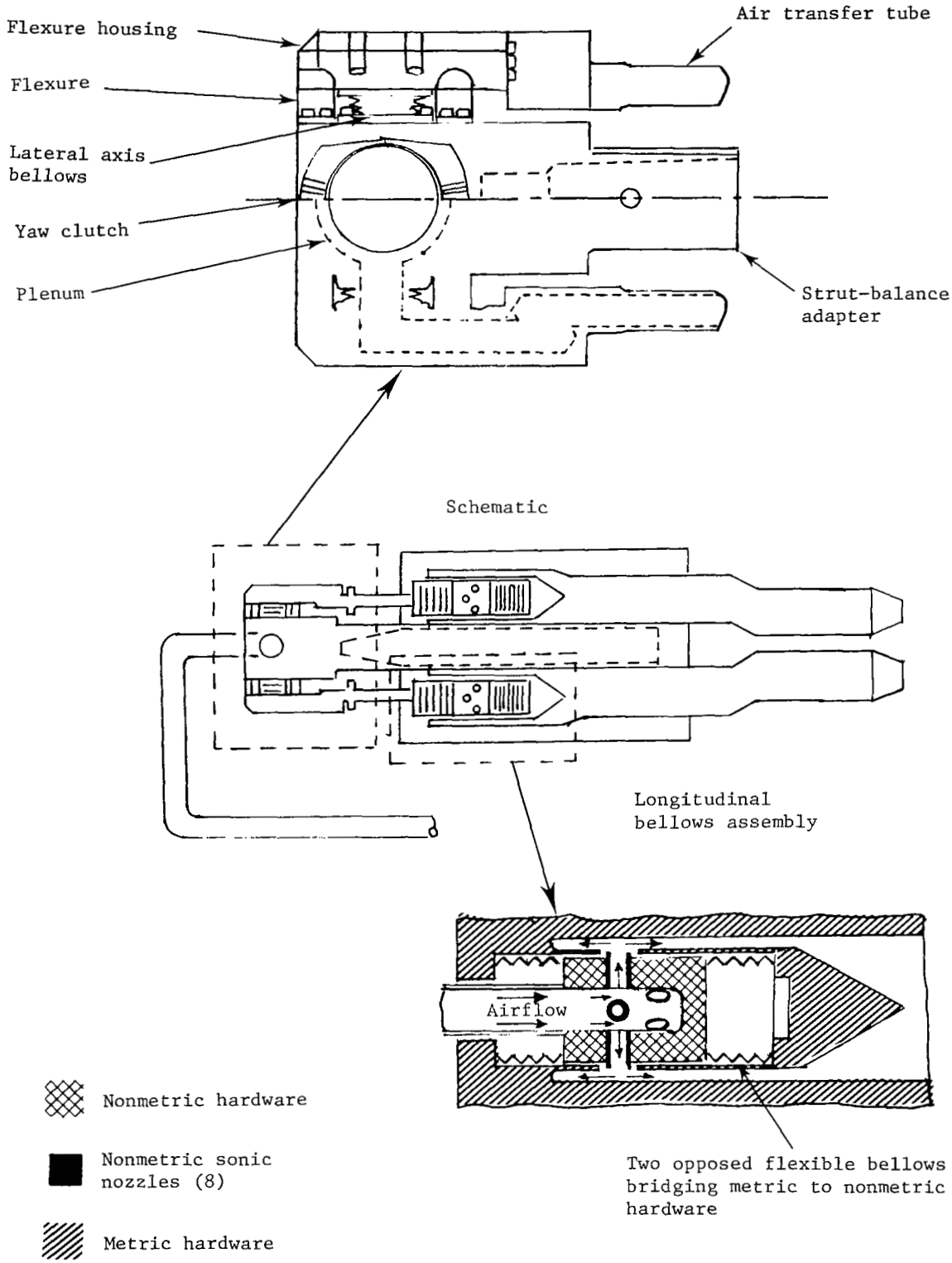

Figure 13.- Air transfer system of F-15 model.

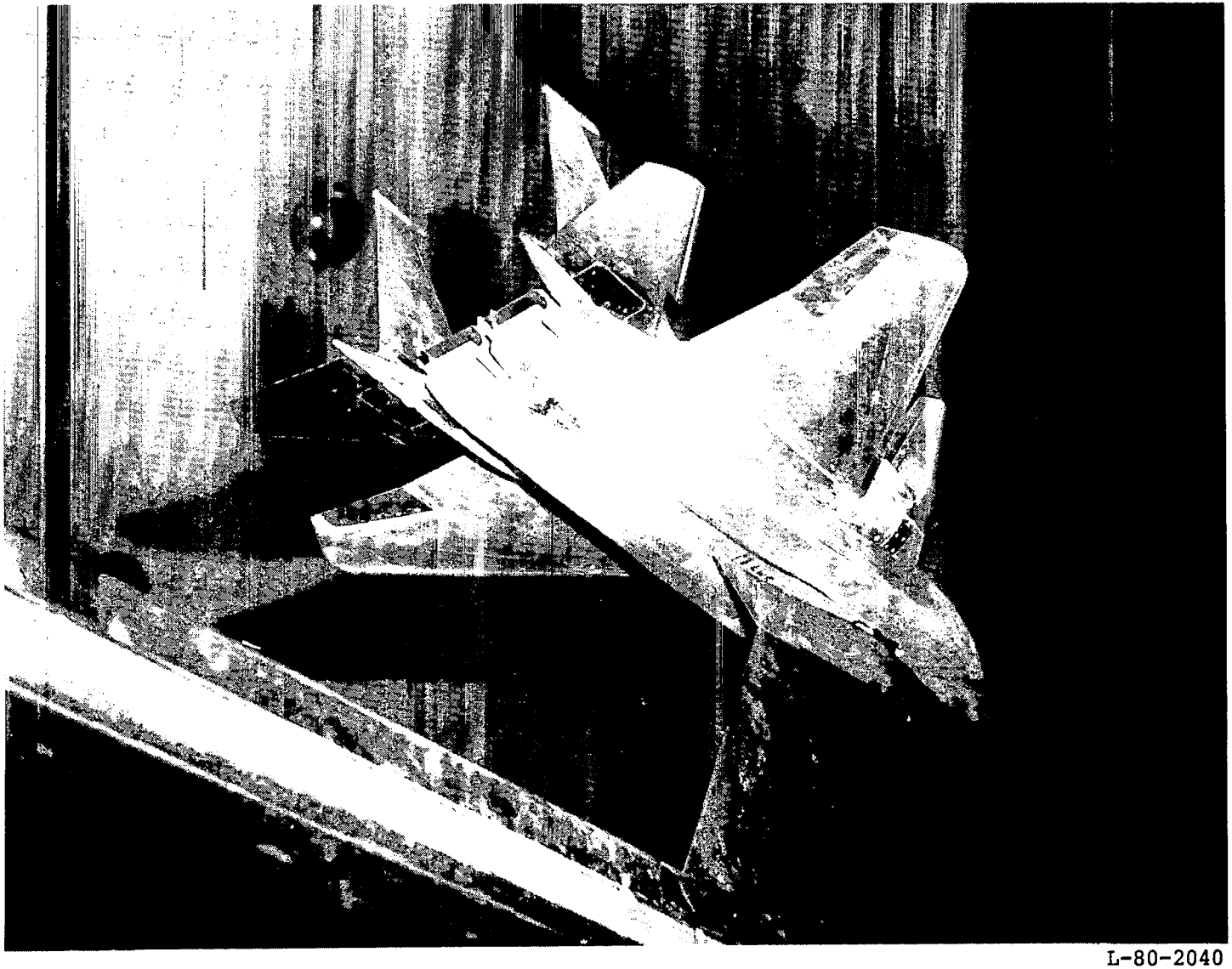

L-80-2040

Figure 14.- Photograph showing 2-D C-D nozzles installed on F-15 three-surface configuration.

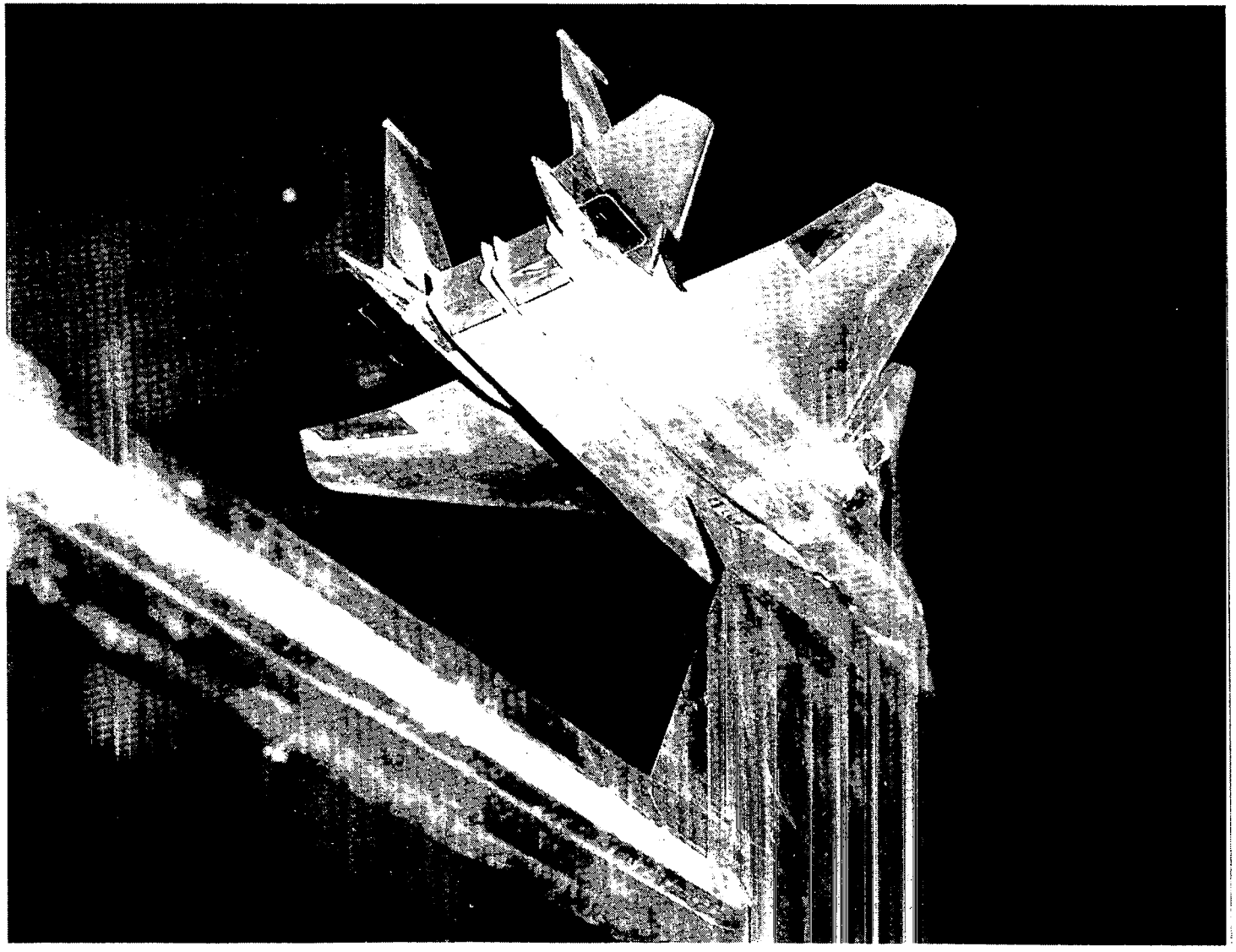

L-80-2671

Figure 15.- Photograph showing 2-D C-D fully deployed thrust reverser installed on F-15 three-surface configuration.

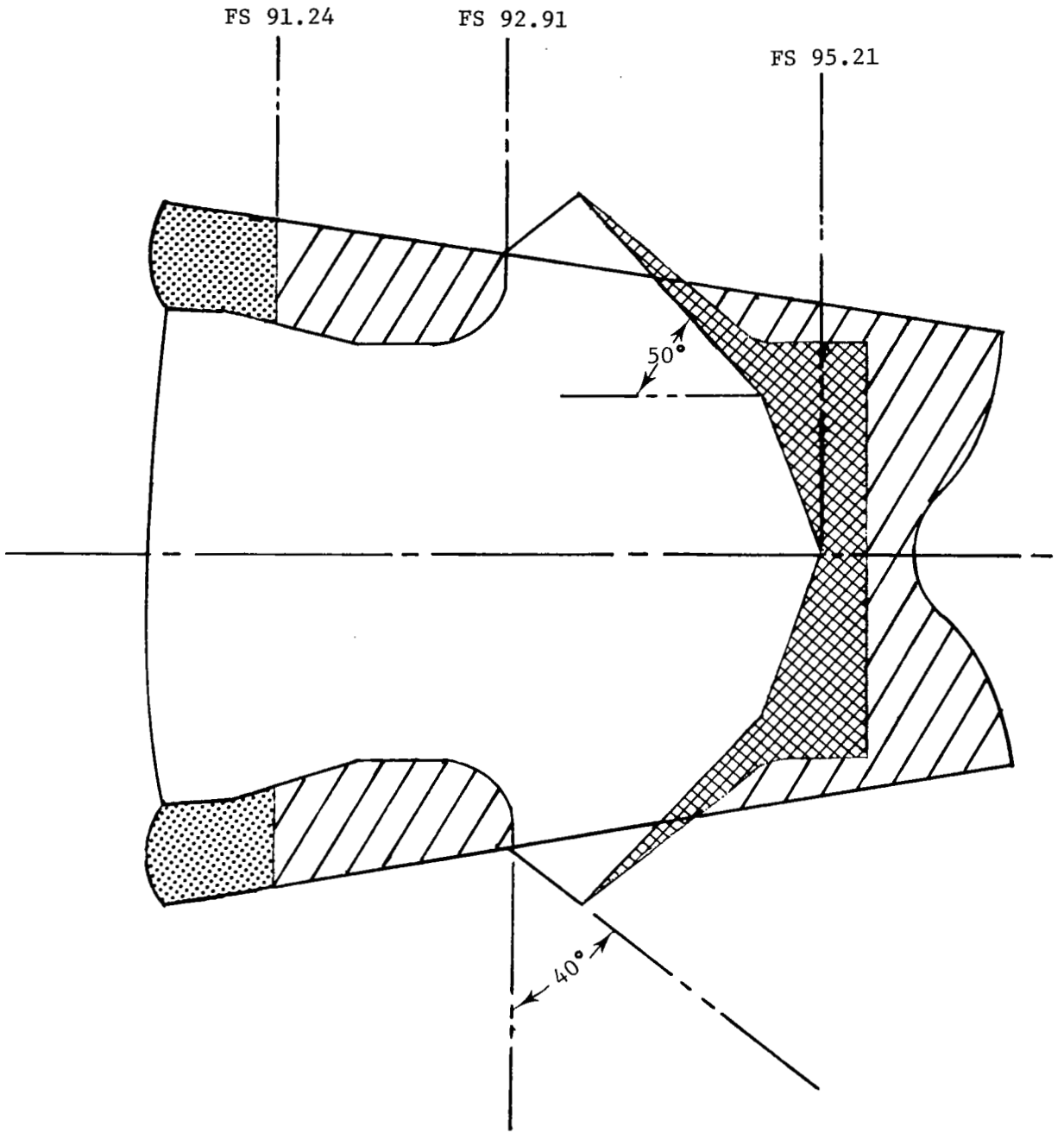

Figure 16.- Sketch showing fully deployed thrust reverser on 2-D C-D nozzle. All dimensions are in centimeters unless otherwise specified.

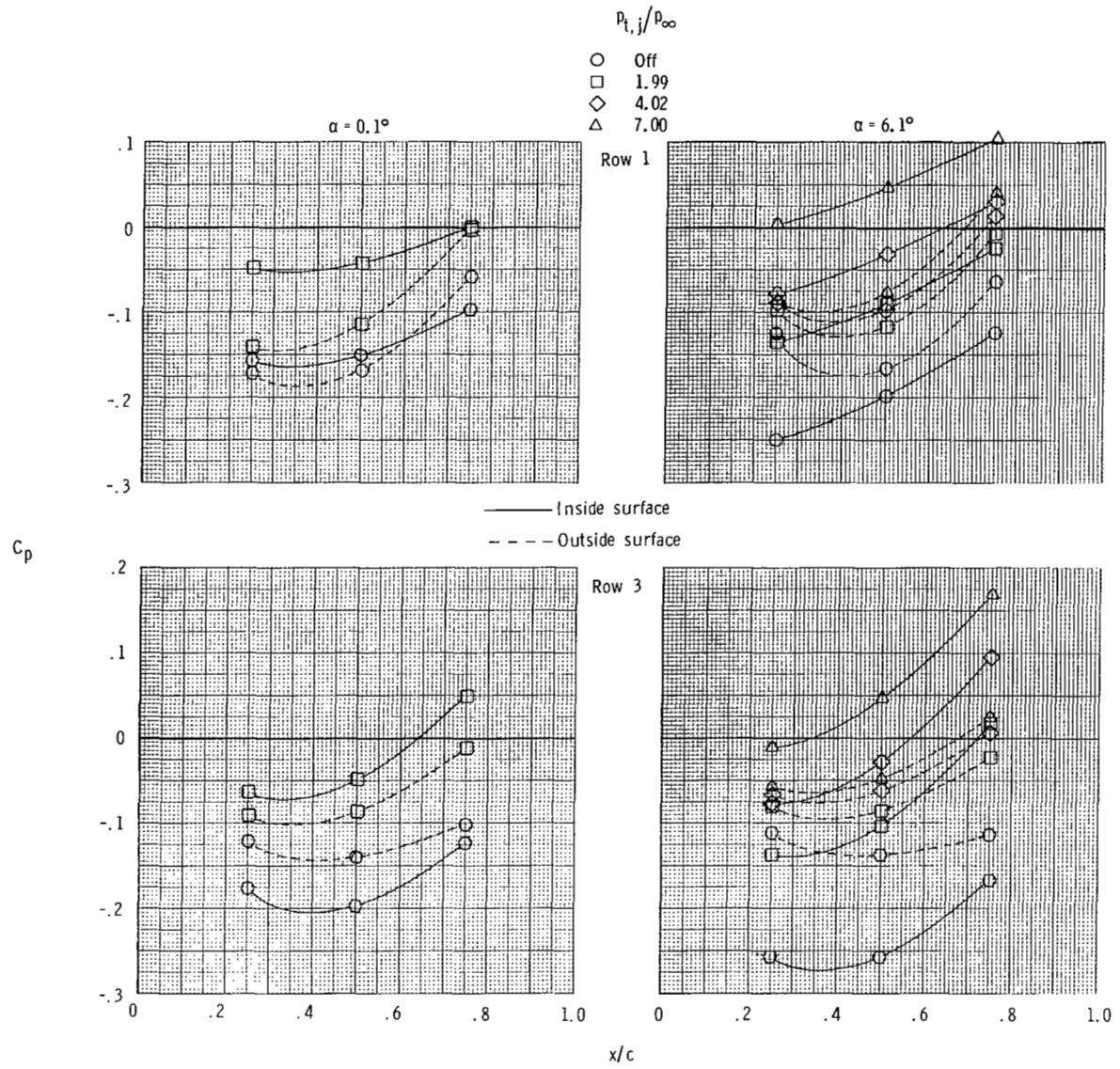

(a) M = 0.6.

Figure 17.- Effect of nozzle pressure ratio, angle of attack, and Mach number on vertical-tail pressure coefficients of 100-percent fully deployed 2-D C-D reverser installed on F-18 model.

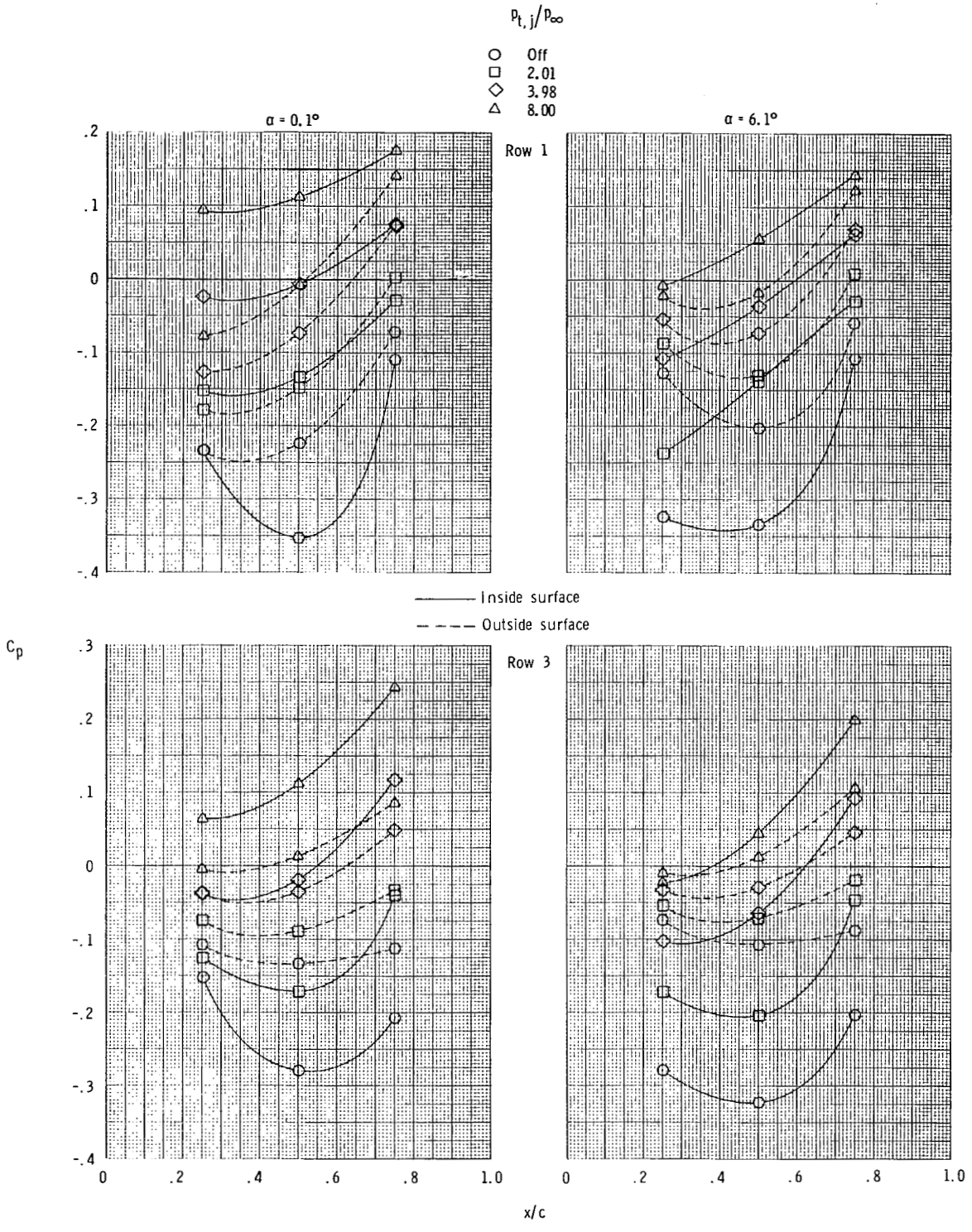

(b) M = 0.9.

Figure 17.- Continued.

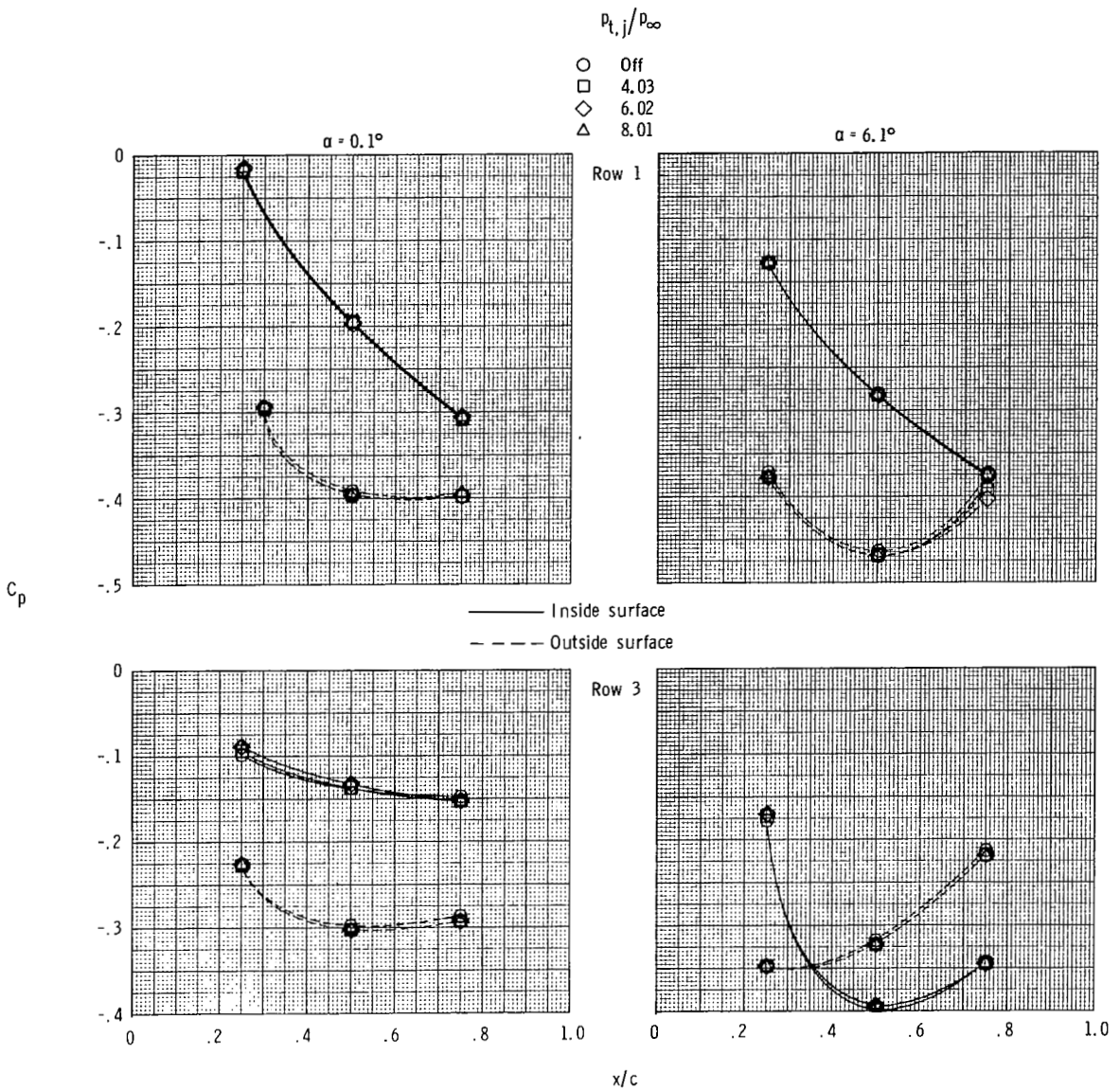

(c) M = 1.2.

Figure 17.- Concluded.

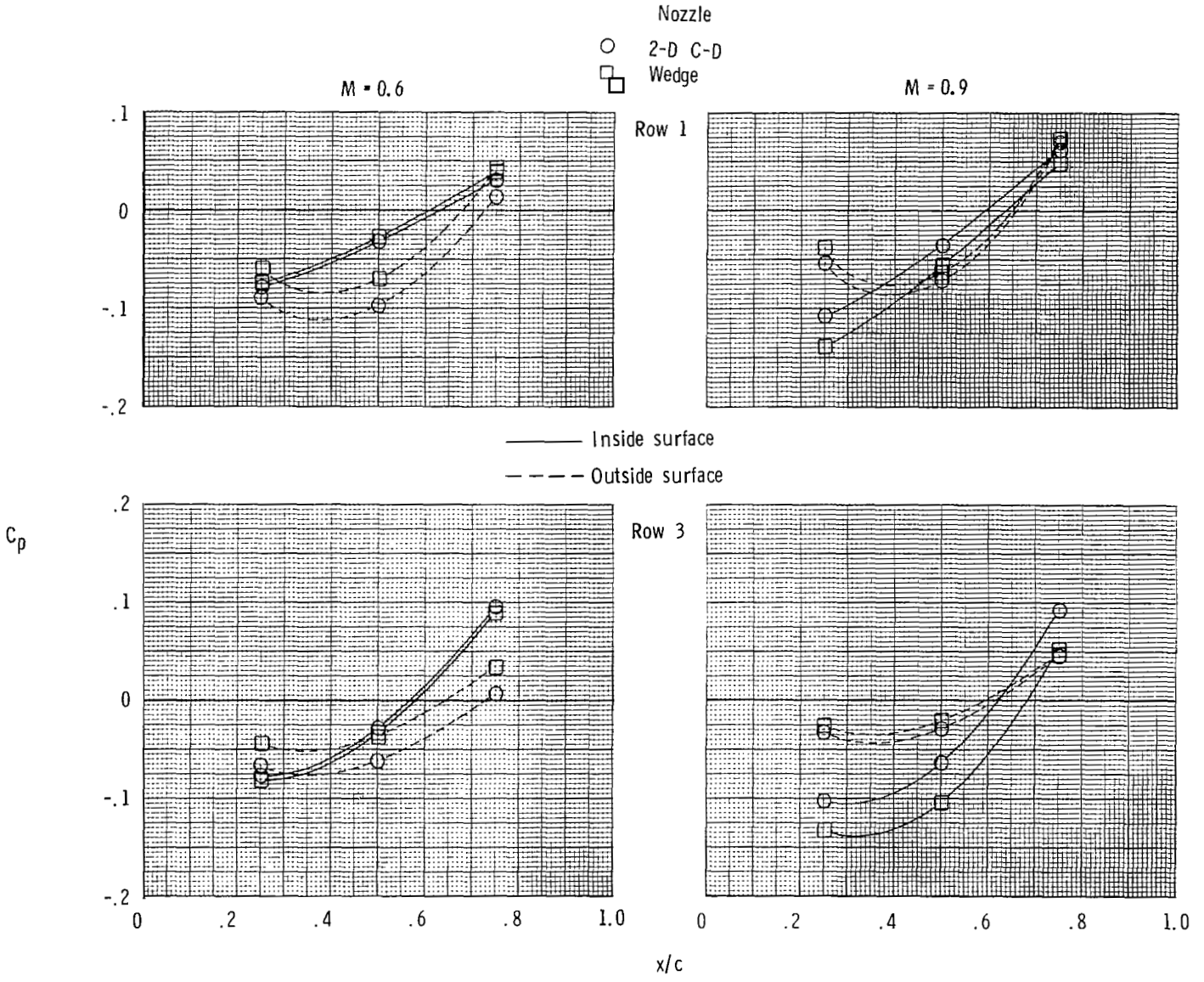

Figure 18.- Effect of nozzle type on vertical-tail pressure coefficients with in-flight reverser fully deployed. F-18 data; $\alpha = 6.1^{\circ}$; $p_{t,j}/p_{\infty} = 4.01$.

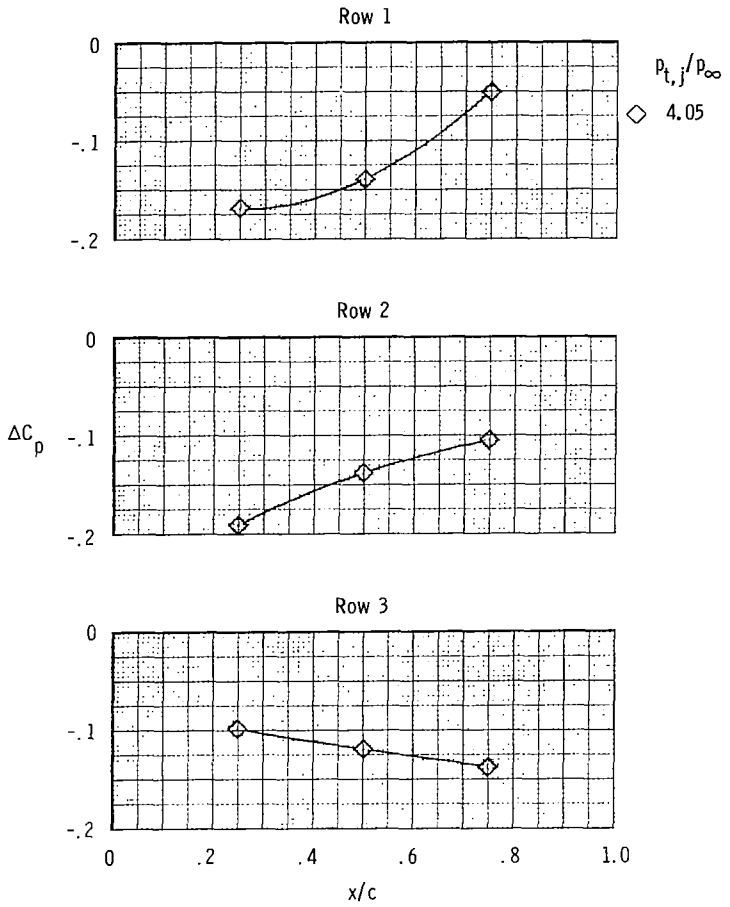

(a) M = 0.6; $\alpha = -1.8^{\circ}$.

Figure 19.- Effect of nozzle pressure ratio, angle of attack, and Mach number on vertical-tail incremental-pressure-coefficient distributions of 100-percent fully deployed 2-D C-D reverser installed on F-18 model.

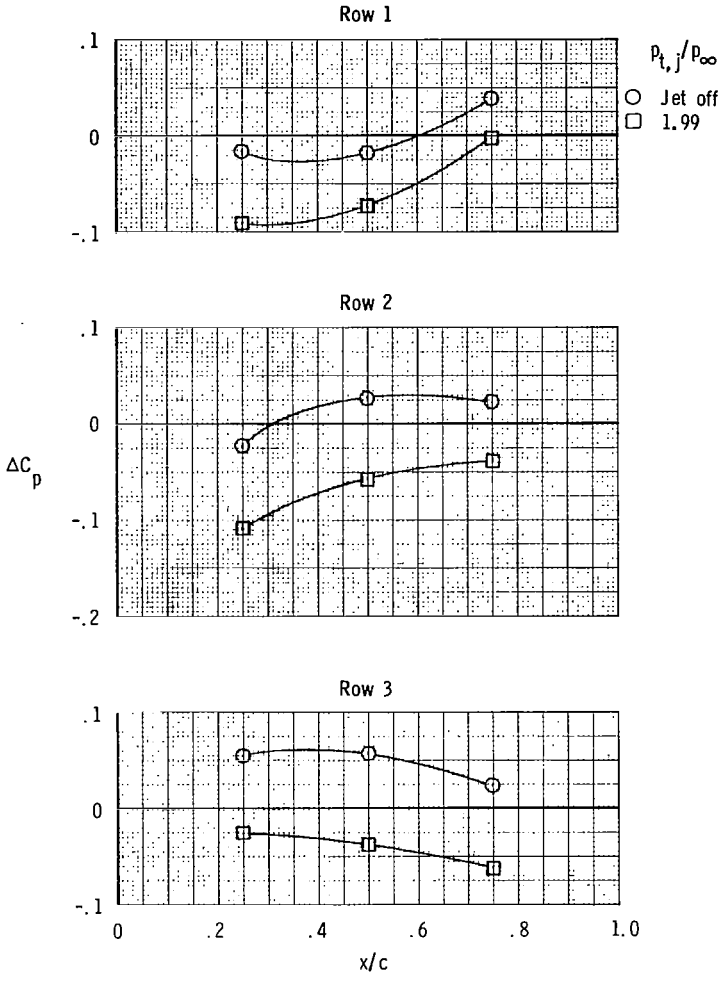

(b) M = 0.6; $\alpha = 0.1^\circ$.

Figure 19.- Continued.

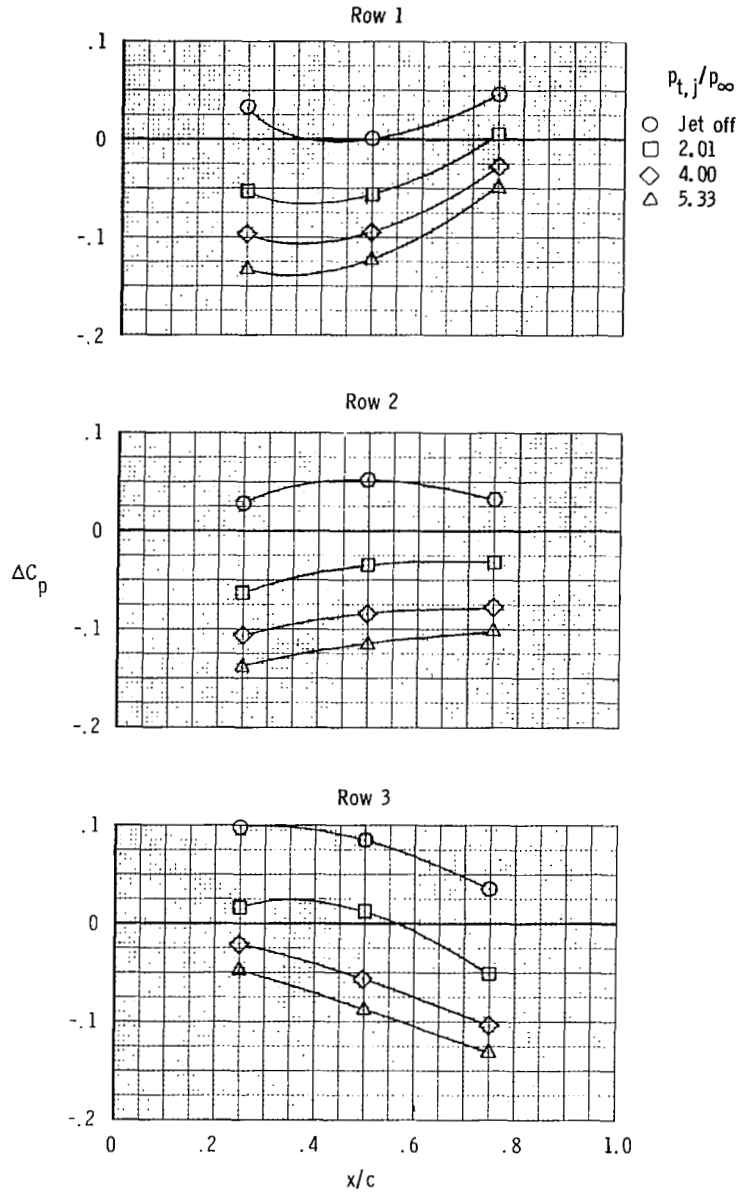

(c) M = 0.6; α = 2.1°.

Figure 19.- Continued.

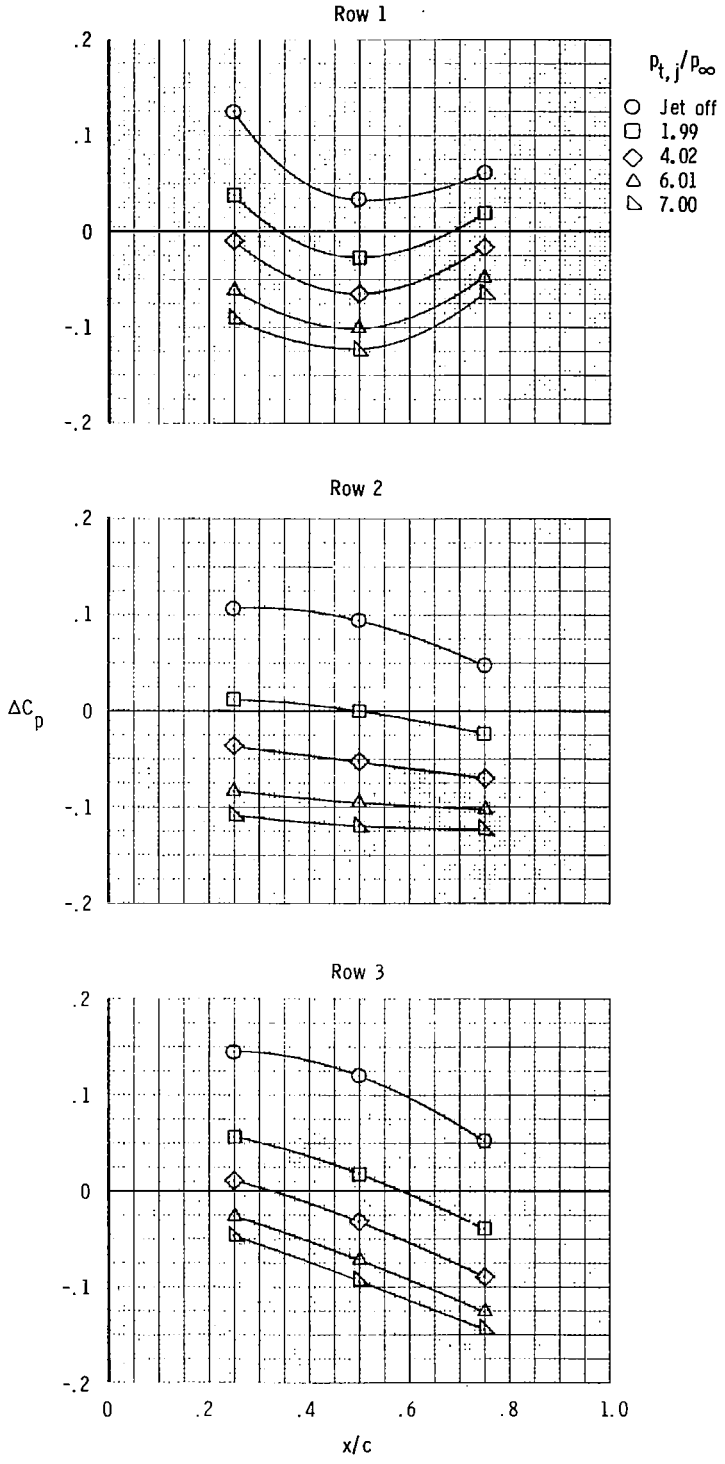

(d) M = 0.6; $\alpha = 6.1^{\circ}$.

Figure 19.- Continued.

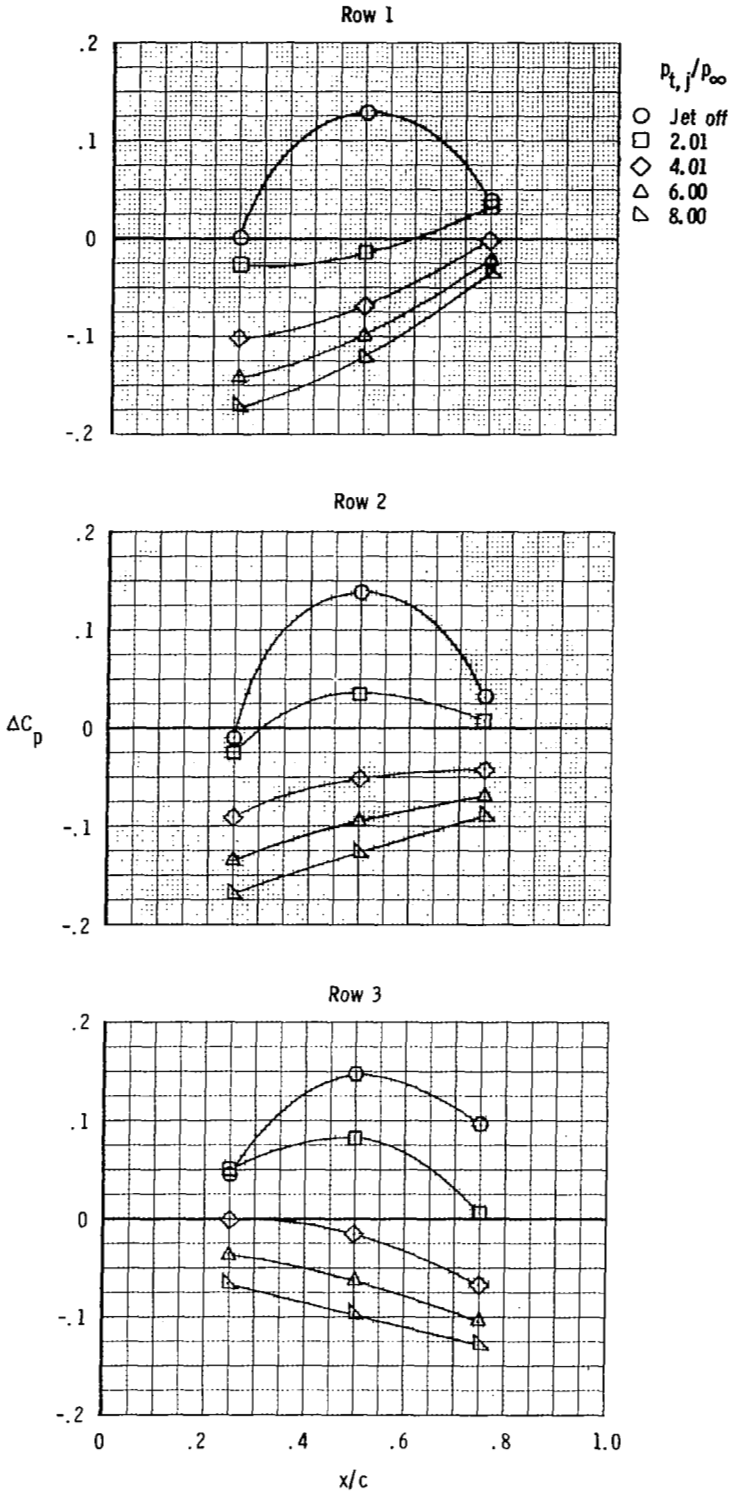

(e) M = 0.9; α = 0.1°.

Figure 19.- Continued.

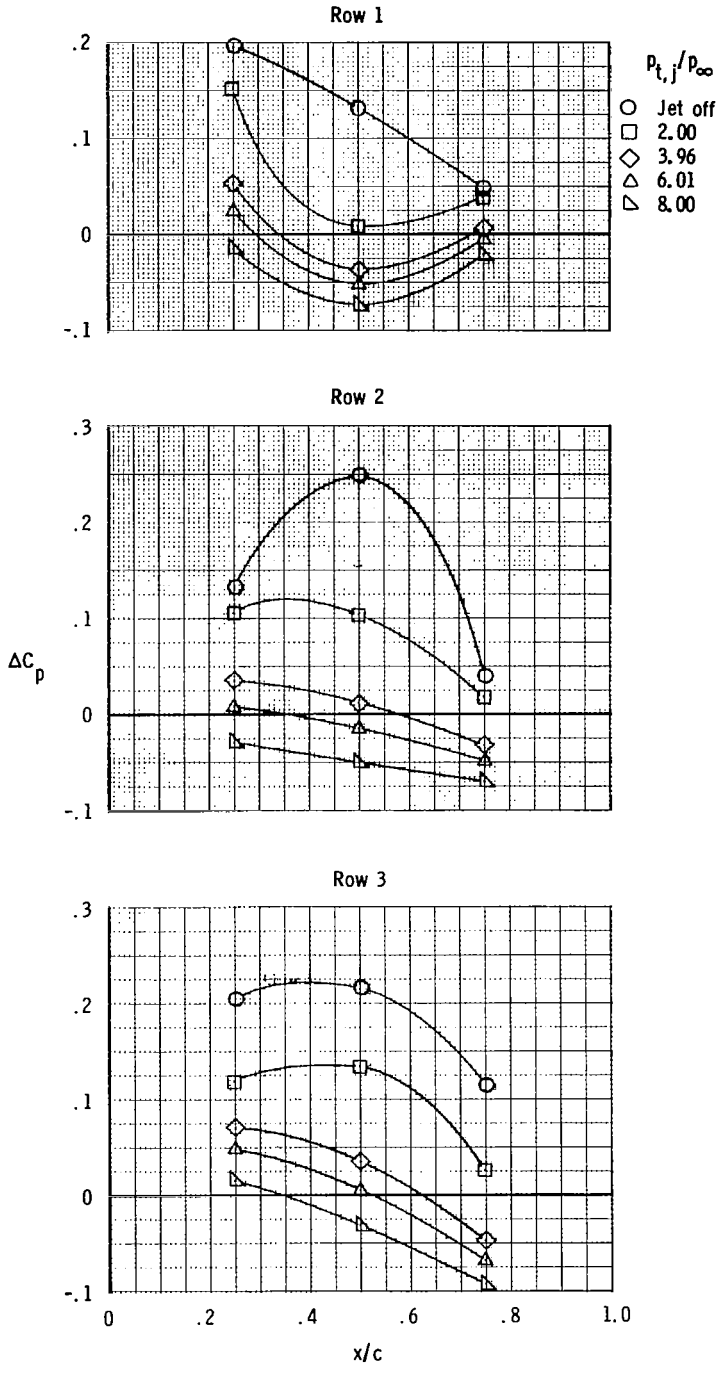

(f) M = 0.9; $\alpha = 6.1^{\circ}$.

Figure 19.- Continued.

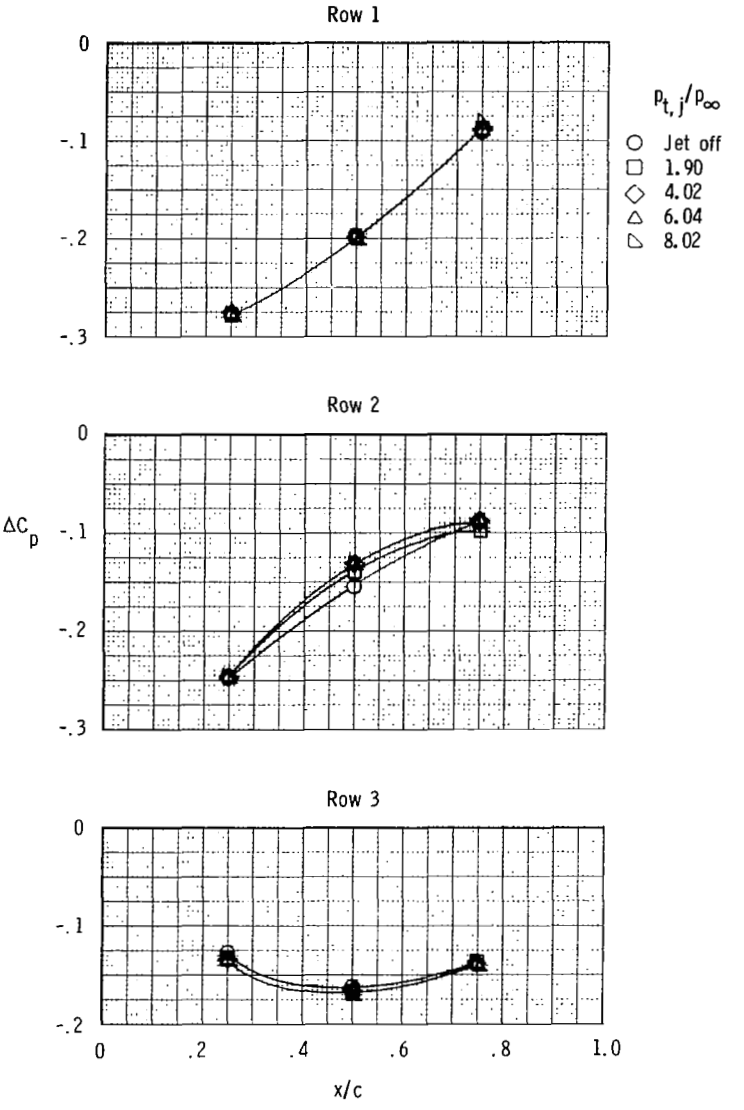

(g) M = 1.2; α = 0.1°.

Figure 19.- Continued.

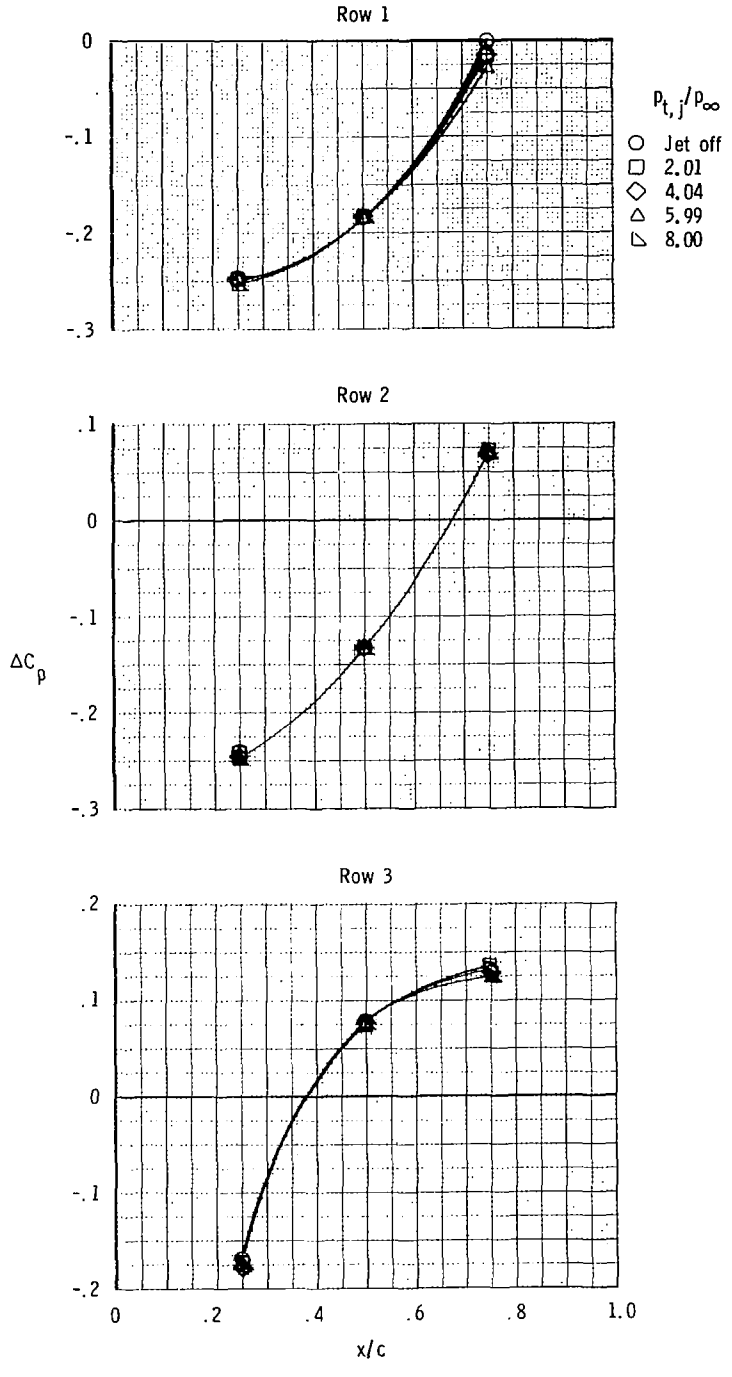

(h) M = 1.2; α = 6.1°.

Figure 19.- Concluded.

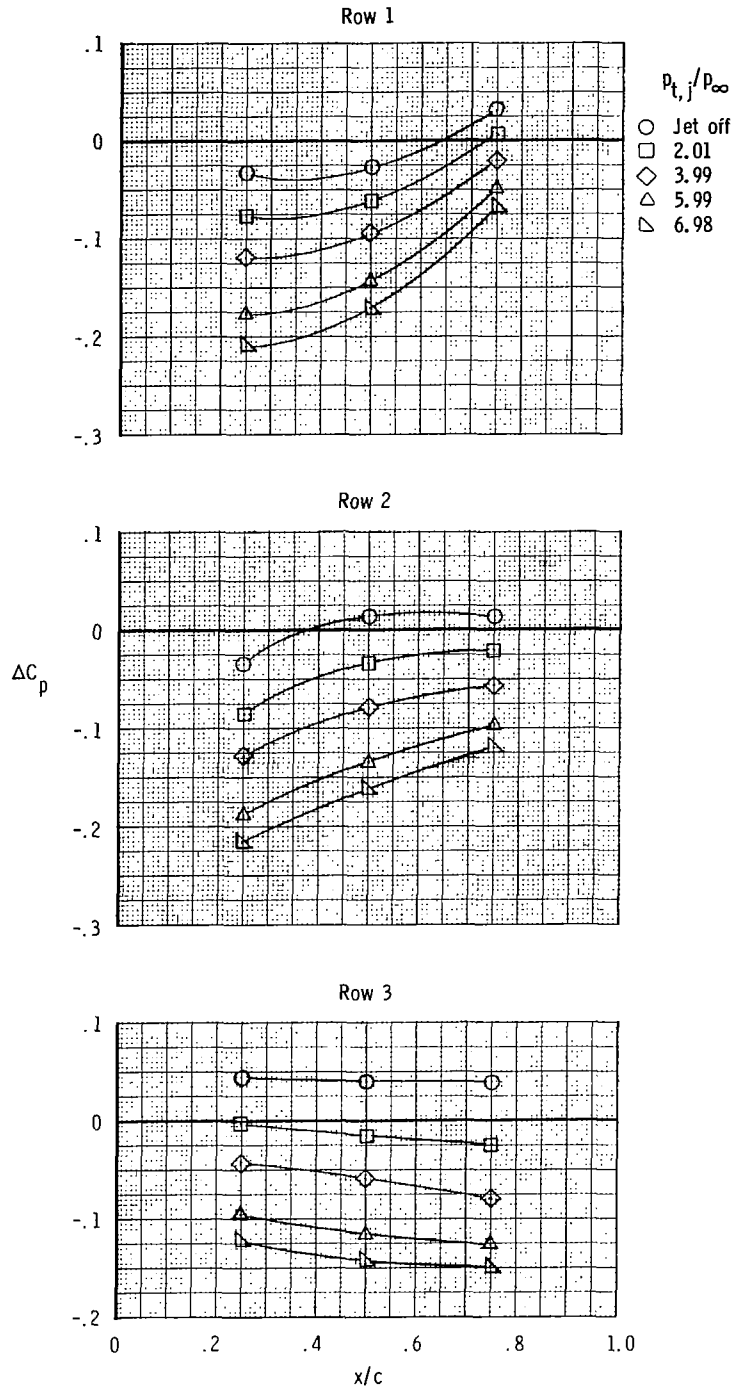

(a) M = 0.6; $\alpha = 0.1^\circ$.

Figure 20.- Effect of nozzle pressure ratio, angle of attack, and Mach number on vertical-tail incremental-pressure-coefficient distributions of 100-percent fully deployed wedge reverser installed on F-18 model.

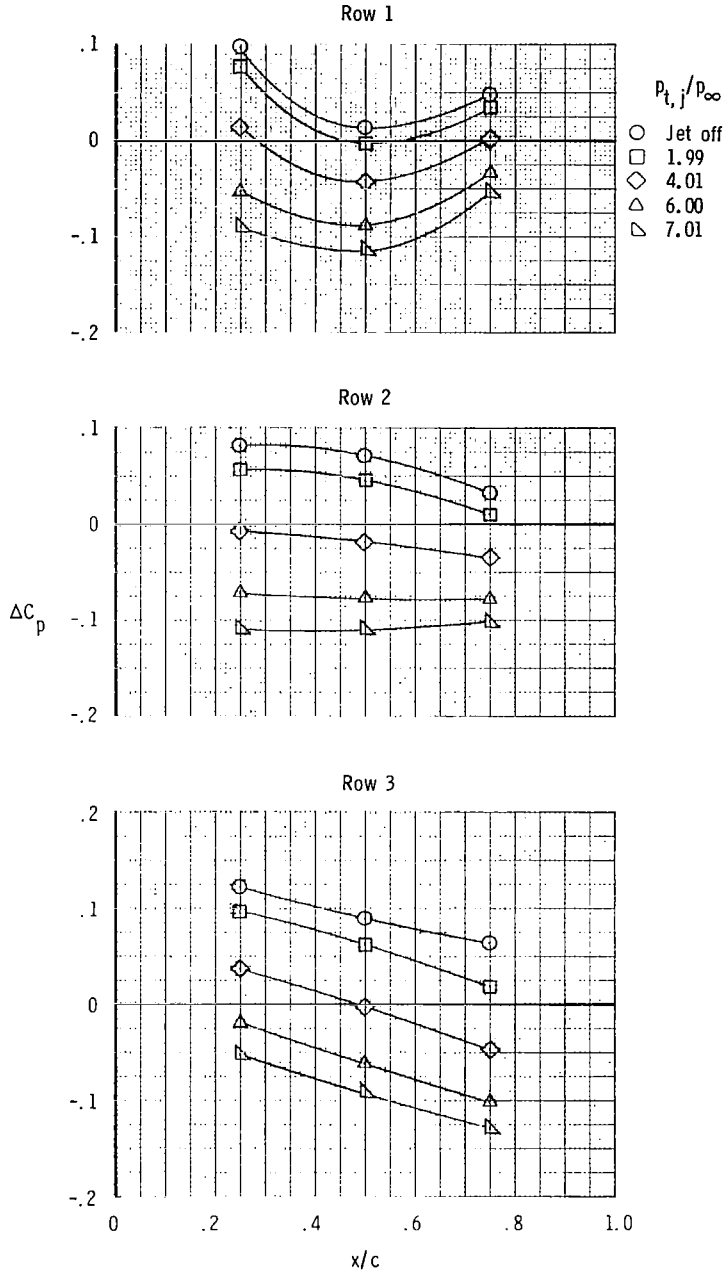

(b) M = 0.6; $\alpha = 6.1^{\circ}$.

Figure 20.- Continued.

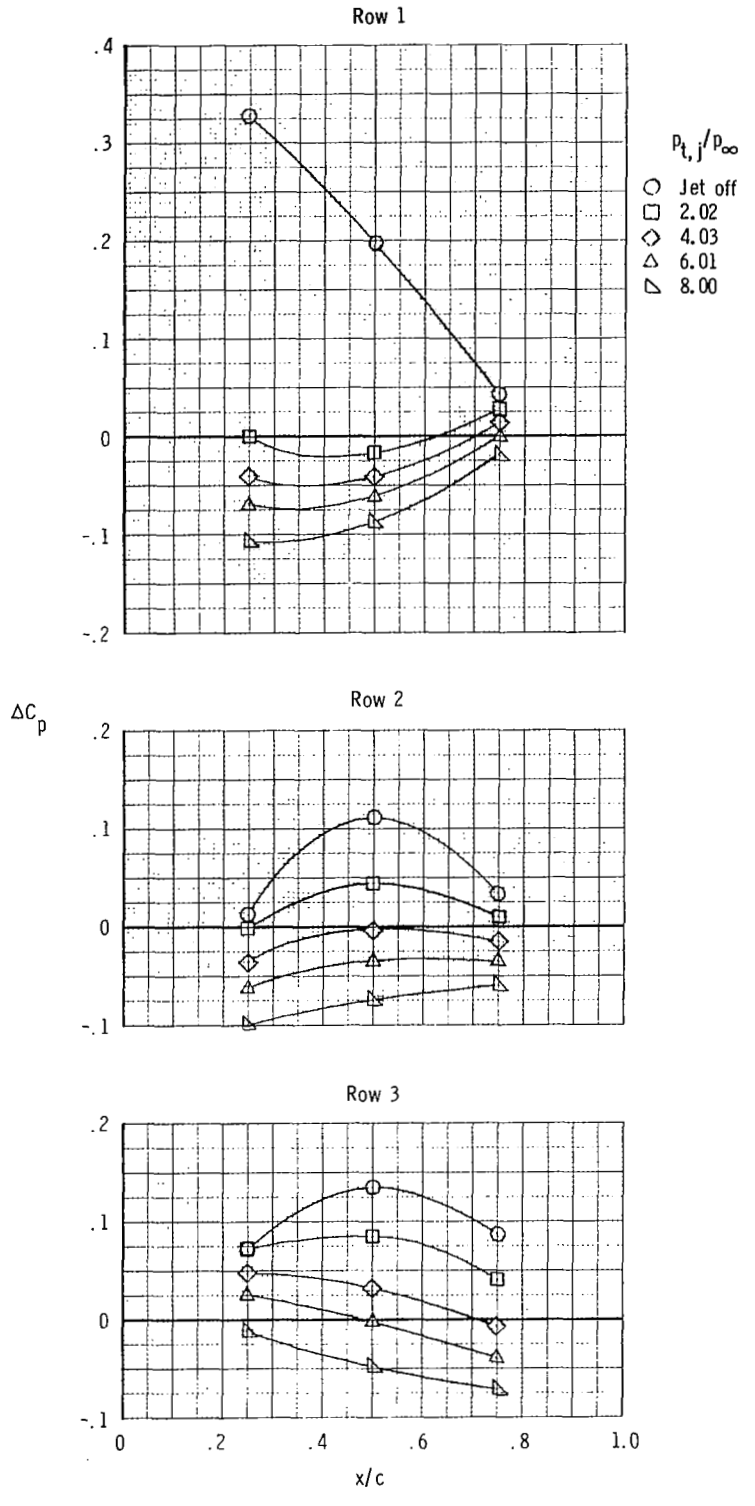

(c) M = 0.9; α = 1.1°.

Figure 20.- Continued.

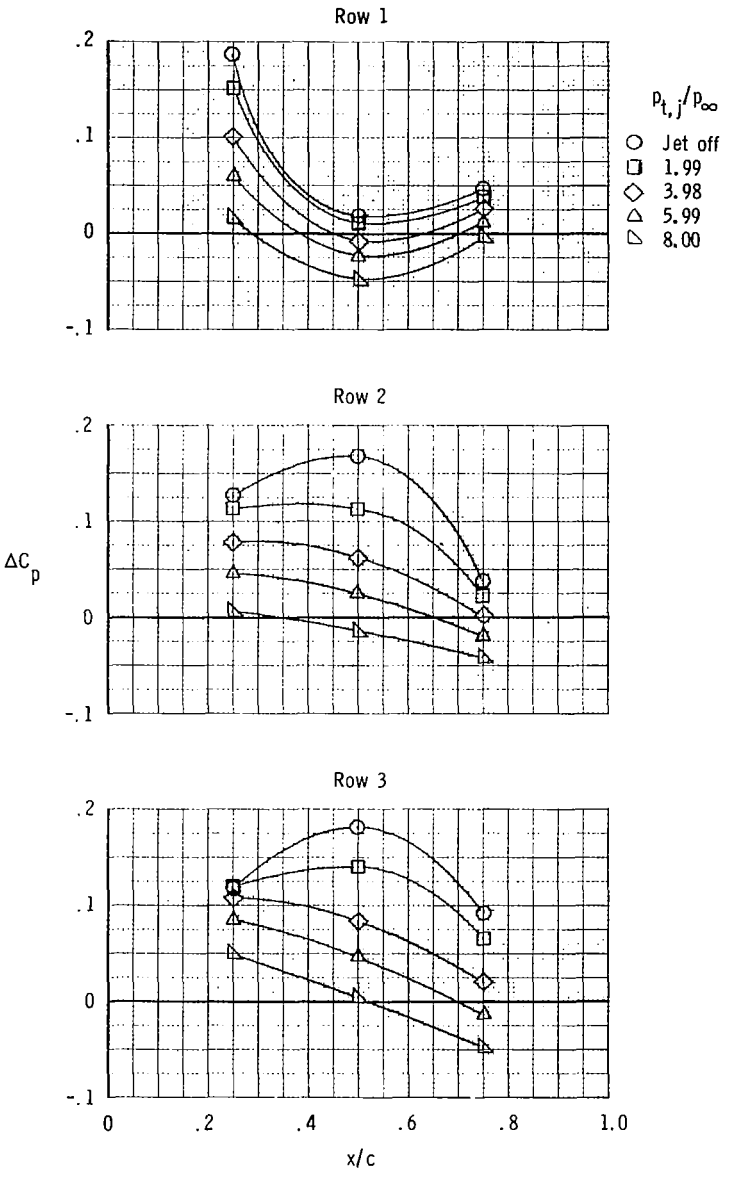

(d) M = 0.9; α = 6.1°.

Figure 20.- Concluded.

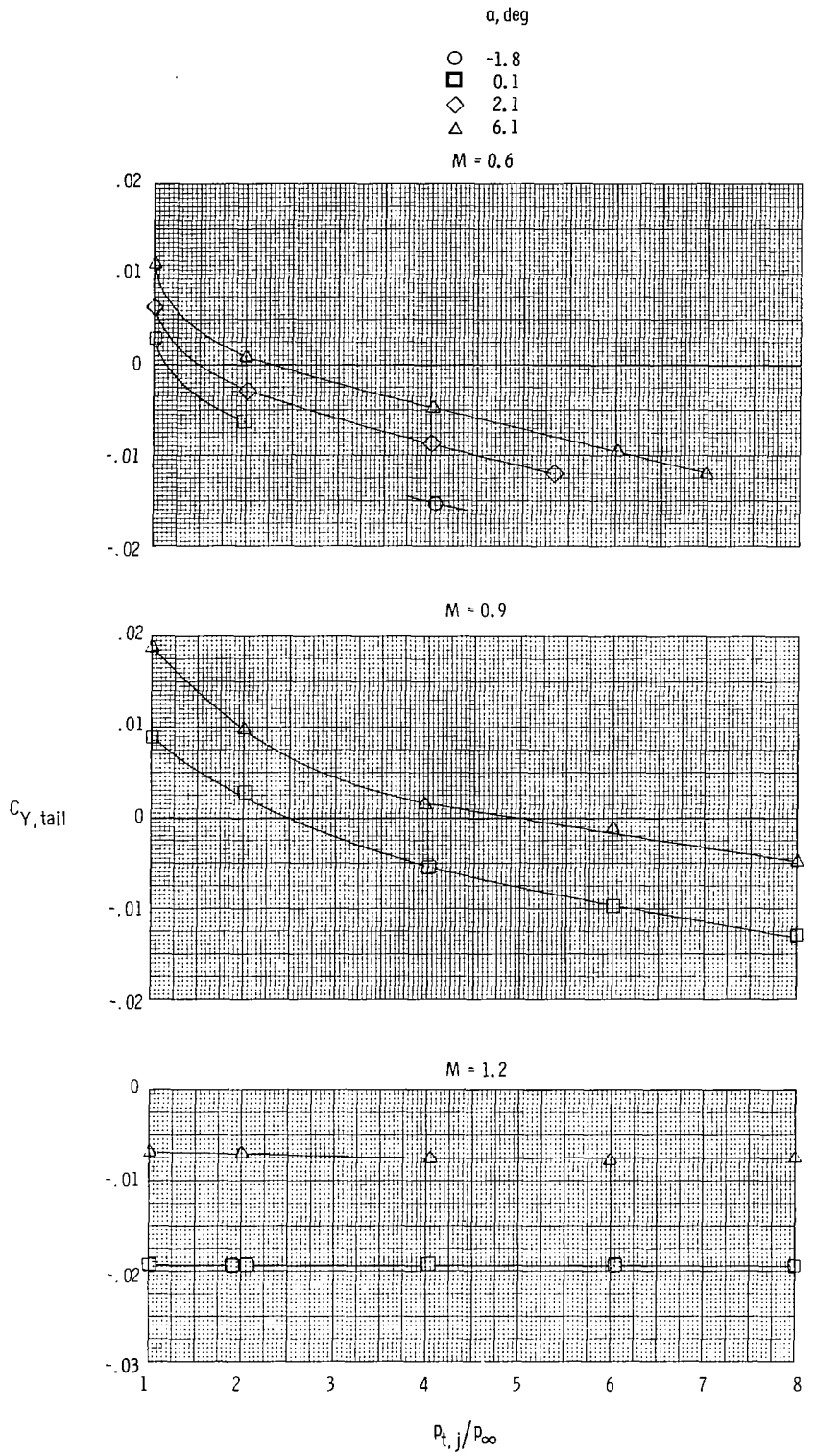

(a) 2-D C-D nozzle.

Figure 21.- Effect of nozzle pressure ratio, angle of attack, and Mach number on vertical-tail side-force coefficient. 100-percent deployed reverser installed on F-18 model.

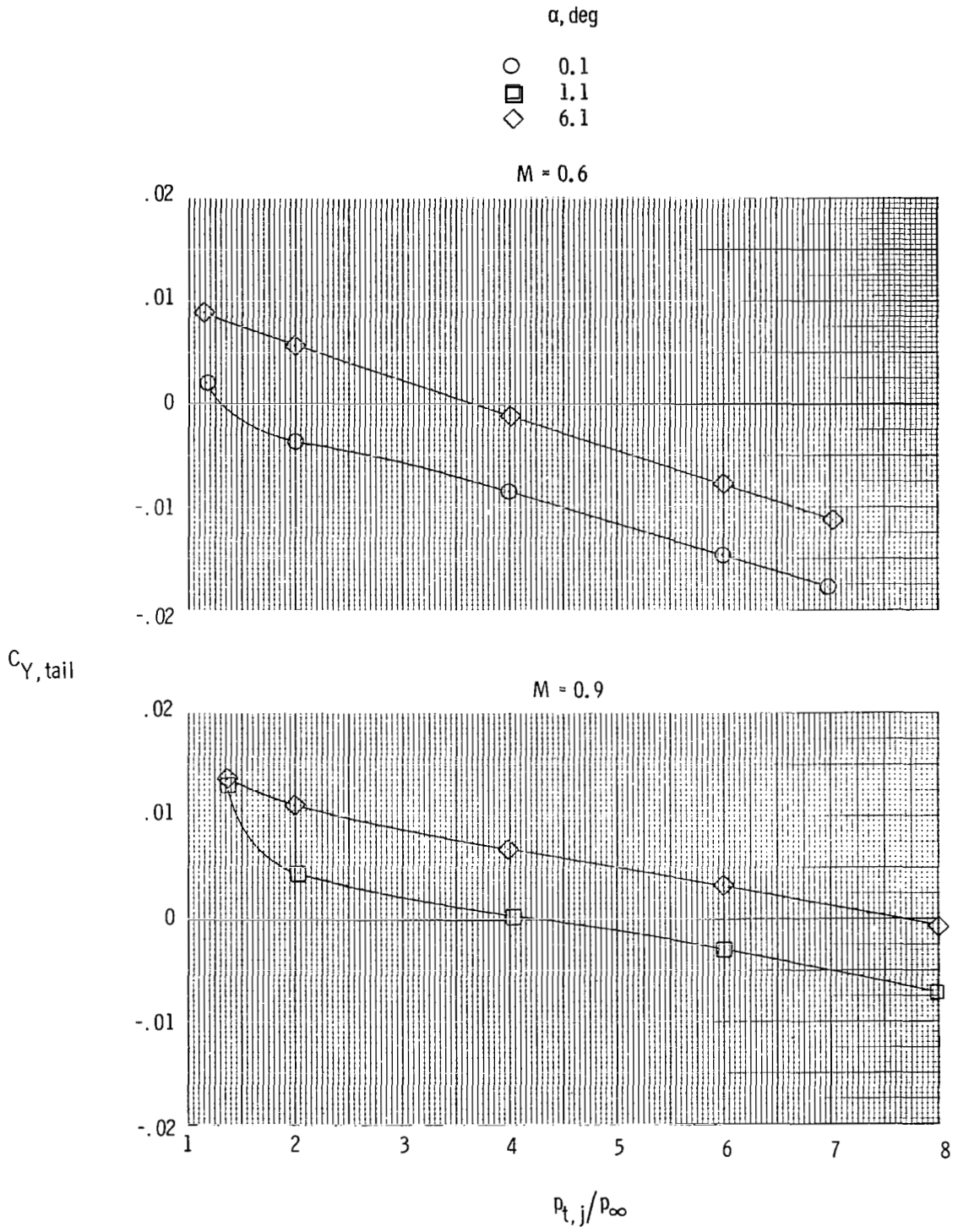

(b) Wedge nozzle.

Figure 21.- Concluded.

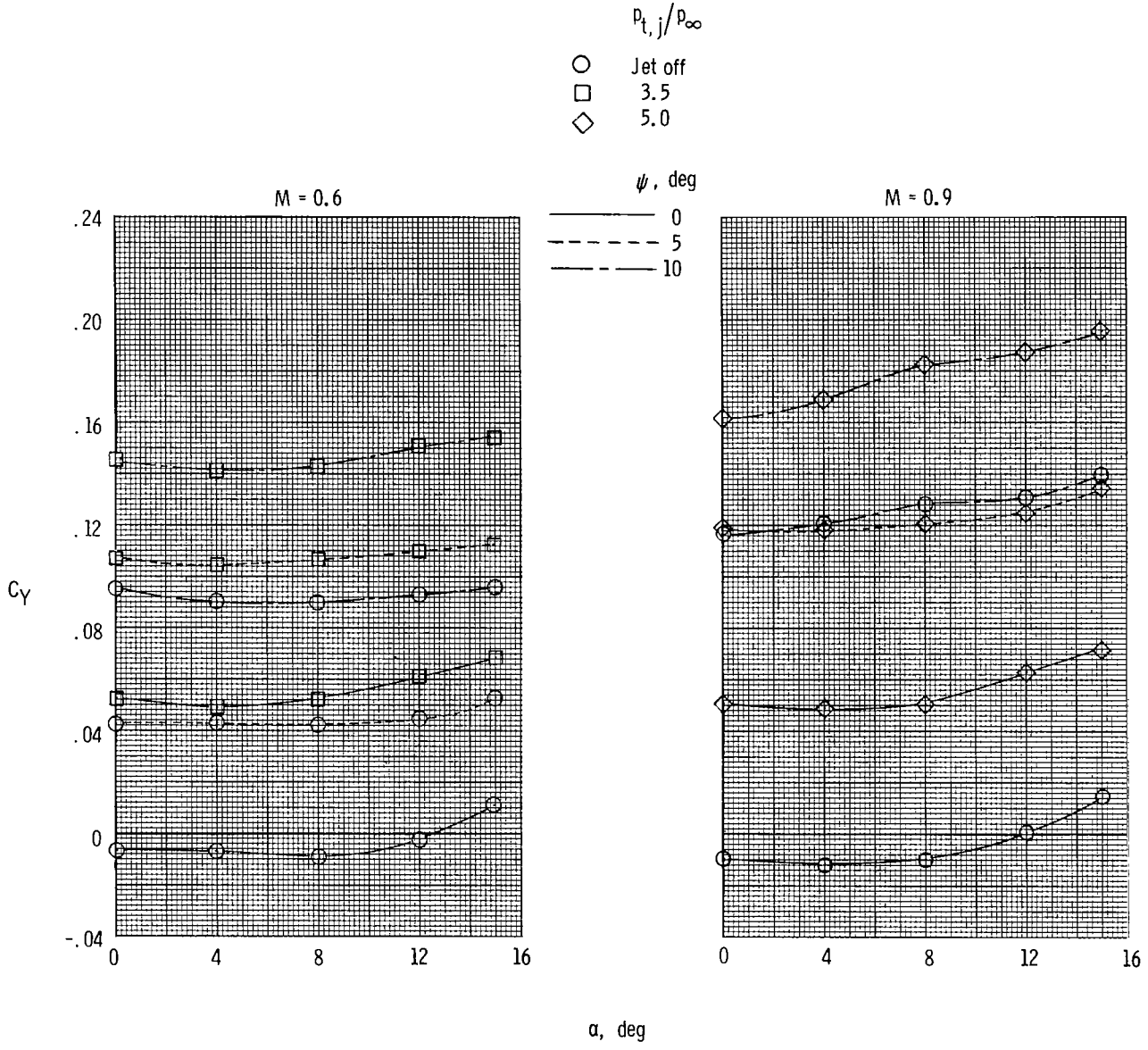

Figure 22.- Effect of nozzle pressure ratio, angle of attack, yaw, and Mach number on total side-force coefficient. 2-D C-D nozzle with fully deployed thrust reverser installed on F-15 model with right-hand vertical tail only.

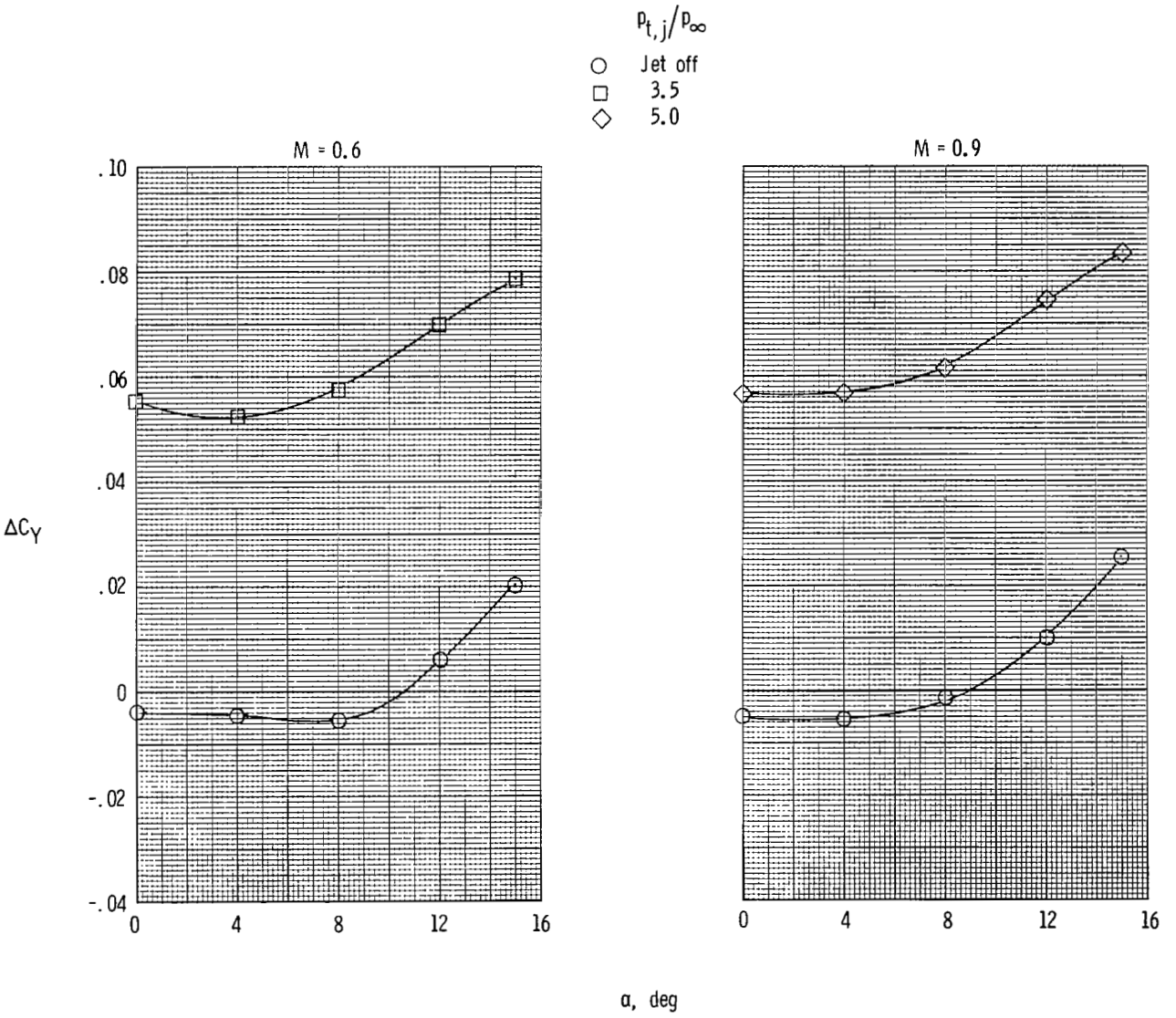

Figure 23.- Effect of nozzle pressure ratio, Mach number, and angle of attack on incremental side-force coefficient. $\psi = 0^o$; 2-D C-D nozzle with fully deployed thrust reverser installed on F-15 model.

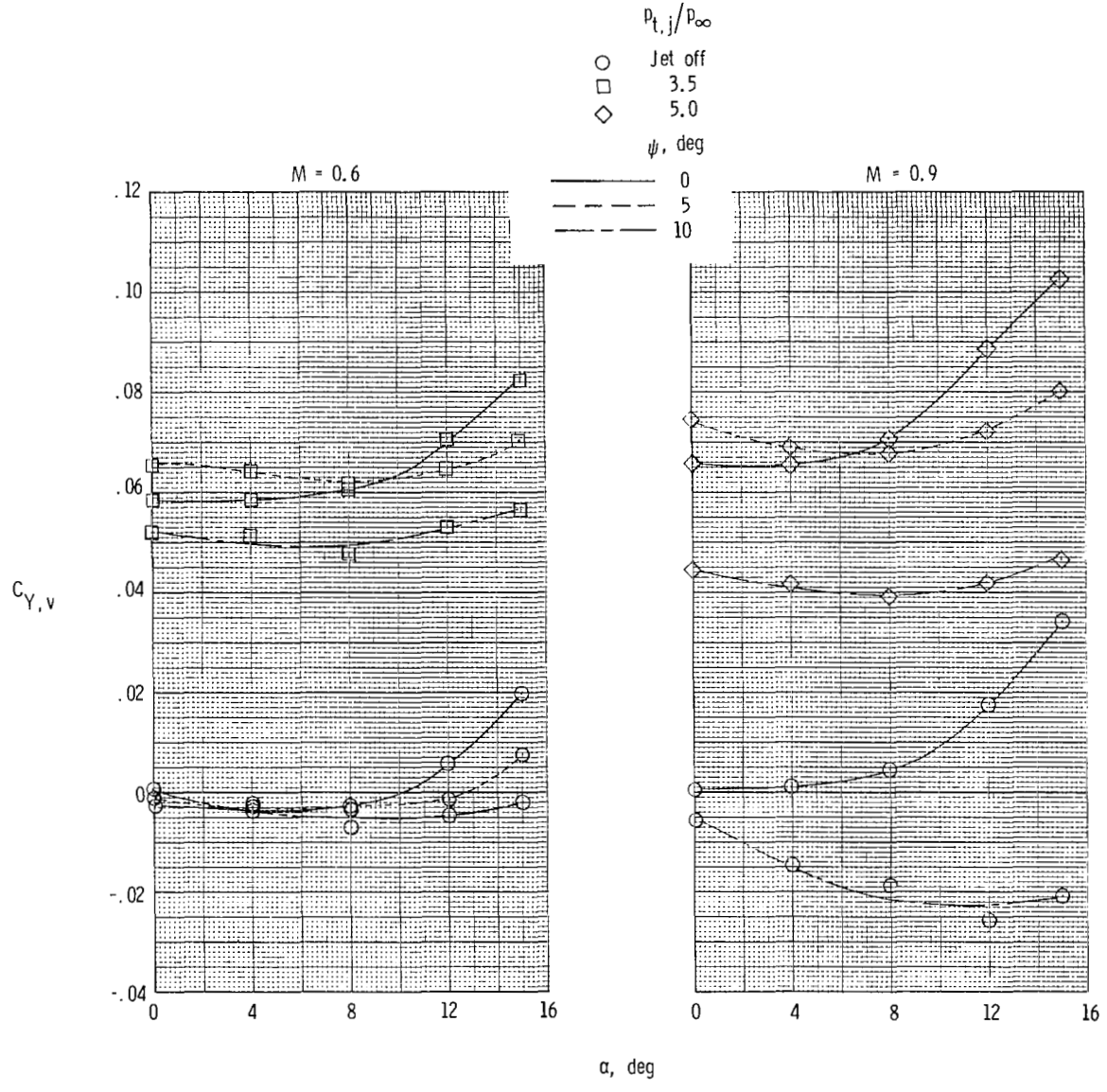

Figure 24.- Effect of nozzle pressure ratio, Mach number, angle of attack, and yaw on vertical-tail side-force coefficient computed from yawing moment. 2-D C-D nozzle with fully deployed thrust reverser installed on F-15 model.

1. Report No.	2. Government Accession No.	3. Recipient's Catalog No.
NASA TP-1890		

4. Title and Subtitle	5. Report Date
EFFECT OF SIMULATED IN-FLIGHT THRUST REVERSING ON VERTICAL-TAIL LOADS OF F-18 AND F-15 AIRPLANE MODELS	August 1981
	6. Performing Organization Code 505-43-23-01

7. Author(s)	8. Performing Organization Report No.
E. Ann Bare, Bobby L. Berrier, and Francis J. Capone	L-14531
	10. Work Unit No.

9. Performing Organization Name and Address	11. Contract or Grant No.
NASA Langley Research Center Hampton, VA 23665	

12. Sponsoring Agency Name and Address	13. Type of Report and Period Covered
National Aeronautics and Space Administration Washington, DC 20546	Technical Paper
	14. Sponsoring Agency Code

15. Supplementary Notes

16. Abstract

Investigations were conducted in the Langley 16-Foot Transonic Tunnel to provide data on the effect of simulated in-flight thrust reversing on vertical-tail loads of a 0.10-scale model of the prototype F-18 airplane and a 0.047-scale model of the F-15 three-surface configuration (canard, wing, and horizontal tails). Test data were obtained at static conditions and at Mach numbers from 0.6 to 1.2 over an angle-of-attack range from -2° to 15°. Nozzle pressure ratio was varied from jet off to about 8.0.

17. Key Words (Suggested by Author(s))	18. Distribution Statement
Nonaxisymmetric nozzles Two-dimensional nozzles Reverse thrust Vertical-tail loads Fighter aircraft	Unclassified - Unlimited Subject Category 02

19. Security Classif. (of this report)	20. Security Classif. (of this page)	21. No. of Pages	22. Price
Unclassified	Unclassified	51	A03

For sale by the National Technical Information Service, Springfield, Virginia 22161

NASA-Langley, 1981